

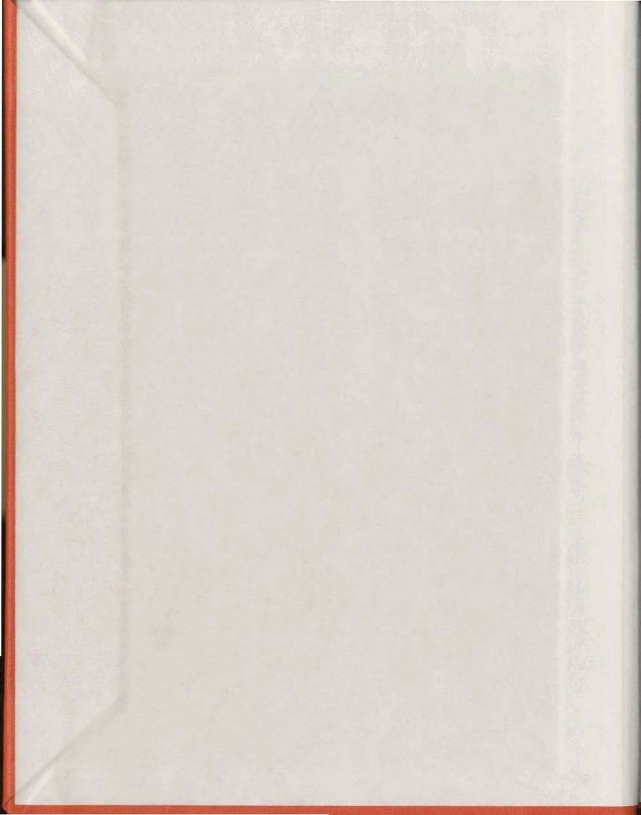
MODELLING OF ICEBERG DRIFT

CENTRE FOR NEWFOUNDLAND STUDIES

**TOTAL OF 10 PAGES ONLY
MAY BE XEROXED**

(Without Author's Permission)

MONA SALAH SHAHWAN EL-TAHAN



000233





National Library of Canada
Collections Development Branch

Canadian Theses on
Microfiche Service

Bibliothèque nationale du Canada
Direction du développement des collections

Service des thèses canadiennes
sur microfiche

NOTICE

The quality of this microfiche is heavily dependent upon the quality of the original thesis submitted for microfilming. Every effort has been made to ensure the highest quality of reproduction possible.

If pages are missing, contact the university which granted the degree.

Some pages may have indistinct print especially if the original pages were typed with a poor typewriter ribbon or if the university sent us a poor photocopy.

Previously copyrighted materials (journal articles, published tests, etc.) are not filmed.

Reproduction in full or in part of this film is governed by the Canadian Copyright Act, R.S.C. 1970, c. C-30. Please read the authorization forms which accompany this thesis.

**THIS DISSERTATION
HAS BEEN MICROFILMED
EXACTLY AS RECEIVED**

AVIS

La qualité de cette microfiche dépend grandement de la qualité de la thèse soumise au microfilmage. Nous avons tout fait pour assurer une qualité supérieure de reproduction.

S'il manque des pages, veuillez communiquer avec l'université qui a conféré le grade.

La qualité d'impression de certaines pages peut laisser à désirer, surtout si les pages originales ont été dactylographiées à l'aide d'un ruban usé ou si l'université nous a fait parvenir une photocopie de mauvaise qualité.

Les documents qui font déjà l'objet d'un droit d'auteur (articles de revue, examens publiés, etc.) ne sont pas microfilmés.

La reproduction, même partielle, de ce microfilm est soumise à la Loi canadienne sur le droit d'auteur, SRC 1970, c. C-30. Veuillez prendre connaissance des formules d'autorisation qui accompagnent cette thèse.

**LA THÈSE A ÉTÉ
MICROFILMÉE TELLE QUE
NOUS L'AVONS REÇUE**

MODELLING OF ICEBERG DRIFT

by



Moná Salah Shahwan El-Tahan

A Thesis submitted in partial fulfillment of the requirements for the
degree of

Master of Engineering

Faculty of Engineering and Applied Science
Memorial University of Newfoundland
St. John's, Newfoundland, Canada

April 1980

To My Parents

ABSTRACT

The need for a numerical model to predict iceberg drift arises primarily due to the hazards that icebergs present to the drilling vessels and platform in the offshore areas near Newfoundland and Labrador.

A dynamic model has been developed and used to study the behaviour of icebergs under different wind and current conditions.

The forces considered are due to wind, current, Coriolis effects, pressure gradients (ocean surface slope) and the acceleration of water body surrounding the iceberg. Two different techniques were used to solve the coupled non-linear differential equations of motions: 1) analog computer simulation and 2) digital computer using 4th-order Runge-Kutta method.

The validity of this model is verified by comparing the predicted and observed iceberg trajectory during a storm on August 21-22, 1972 when an oceanographic study, conducted by the Faculty of Engineering and Applied Science of Memorial University of Newfoundland, was in progress near Saglek, Labrador to monitor iceberg positions with the help of radar. The detailed wind and current data measured in-situ near the icebergs, provided a unique opportunity to verify the model and to study the effect of each of the environmental forces. Several trajectories are obtained after excluding each one of the environmental forces used in the model in order to appreciate its effect on the drift of icebergs.

In an attempt to obtain better understanding of the observed looping and spiral motions of icebergs, several trajectories are plotted

for icebergs drifting under the environmental conditions thought to be responsible for this strange behaviour. Changes in the ocean surface due to low pressure systems were found, using finite element analysis, to have no effect on the currents, and hence on the iceberg trajectory.

This study has demonstrated the importance of each of the environmental forces included in the model. A good prediction of an iceberg drift trajectory is only possible if all the environmental forces are accounted for and detailed wind and current data in the immediate vicinity of the iceberg as well as good estimates of iceberg parameters are available as input to the model.

ACKNOWLEDGEMENT

The author wishes to express her sincere thanks to Prof. D.S. Sodhi, Faculty of Engineering and Applied Science, for his guidance, encouragement and review of the manuscript.

The valuable advice and help provided by Prof. M. Booton during the sabbatical leave of Prof. Sodhi is gratefully acknowledged.

The author would like to express her appreciation to Dean R.T. Dempster for making available the iceberg data and for his encouragement.

The author is grateful to Dr. Miles McPhee of U.S. Army Cold Regions Research and Engineering Laboratory, Hanover, N.H., for his discussion which led to the successful completion of this work.

Special thanks are due to Dean Aldrich, School of Graduate Studies for providing the financial assistance.

Prof. M. El-Hawary provided valuable advice and help during analog computer programming.

The author is grateful to Mr. N. Riggs, NOROCO Ltd., St. John's, for supplying important reference material and other information.

Finally, the author would like to thank all the faculty members who acted as chairmen of the Graduate Studies Committee during her graduate studies, for their advice and encouragement, and other faculty members whose help made this study possible.

Partial support of this study from the NRC Research Grant No. A8671 is gratefully acknowledged.

TABLE OF CONTENTS

	Page
ABSTRACT	iv
ACKNOWLEDGEMENT	vi
LIST OF TABLES	ix
LIST OF FIGURES	x
 CHAPTER I. INTRODUCTION	
1.1 Background	1
1.2 Iceberg Hazards to Offshore Operations	2
1.3 Statement of the Problem	3
1.4 Thesis Outline	4
 CHAPTER II. REVIEW OF LITERATURE	
2.1 Field Studies	5
2.2 Theoretical Studies	7
2.3 Experimental Work	9
 CHAPTER III. ICEBERG DRIFT MODEL	
3.1 Mathematical Model	10
3.2 Parameters of the Iceberg Under Study	13
 CHAPTER IV. RESULTS	
4.1 Introduction	16
4.2 Drift of an Iceberg Starting From Rest in a Uniform Current	16
4.3 Study of an Iceberg Trajectory Near Saglek	18

	Page
4.4 Results	26
4.5 Discussion of Results	27
CHAPTER V. CONCLUDING REMARKS	29
TABLES AND FIGURES	30
APPENDIX A: ANALOG COMPUTER SIMULATION AND SOME PRACTICAL APPLICATIONS	
A.1 Introduction	45
A.2 Techniques of Analog Computer Simulation	45
A.3 Practical Applications	48
APPENDIX B: EFFECT OF ATMOSPHERIC PRESSURE SYSTEM ON OCEAN CURRENTS INDUCED BY CHANGES IN SEA LEVEL	
B.1 The Equation of Motion	58
B.2 Pressure Distribution	59
B.3 Practical Applications	59
B.4 Discussion and Conclusion	61
REFERENCES	70

LIST OF TABLES

Table	Page
1. Iceberg Characteristics	31
2. Wind Data (from the Log Books of C.S.S. Dawson)	32

LIST OF FIGURES

Figure	Page
1-1 Drift Pattern of Icebergs Offshore Saglek Before Pressure Disturbance	33
1-2 Drift Pattern of Icebergs After Pressure Disturbance	34
4-1 Drift of an Iceberg in Non-Dimensional Coordinates Due to Geostrophic Current For Different Values of TAD^2/F . Curves are Marked at Equal Intervals of T^1	35
4-2 Drift Pattern of Icebergs Offshore Saglek After the Storm in August, 1972 Showing Locations of Current Meters	36
4-3 Predicted and Observed Trajectories of Iceberg No. 20C During the Storm Which Passed Over the Labrador Sea on August 21-22, 1972	37
4-4 Effect of Wind Forces on Iceberg Drift	38
4-5 Iceberg Drift in Geostrophic Current With Inclusion and Exclusion of Wind	39
4-6 Effect of Iceberg Size on the Predicted Trajectory	40
4-7 Predicted Iceberg Drift With Inclusion and Exclusion of Water Acceleration	41
4-8 Effect of Coriolis Force on Iceberg Drift	42
4-9 Effect of Considering the Distribution of the Wind Generated Current Velocity Follows Ekman's Spiral on Predicted Iceberg Drift	43
4-10 Effect of Considering the Distribution of the Wind-Generated Current Velocity	44
A-1 Analog Computer Simulation of Iceberg Motion	50
A-2 Effect of Coriolis Force and Ocean Slope on Iceberg Drift Due to Geostrophic Current of 0.35 m/sec	51
A-3 Iceberg Drift Due to Rotary Current Plus a Translatory Component of 0.085 m/s Period of Rotary Current = 12 hrs	52
A-4 Iceberg Drift for Different Values of K . In a Horizontal Current $U_c = U_0 \sin(\omega t)$	53
A-5 Iceberg Drift Under Coriolis Force Only for Different Initial Velocity U_0	54

Figure	Page
A-6 Effect of K on the Inertial Motion of Iceberg	55
A-7 Iceberg Drift Due to Inertial Current, Current Period = 12 hrs	56
A-8 Iceberg Drift Due to Rotary Current for Two Icebergs With Draughts Less and Greater Than the Depth of Friction Layer D , $UK = 0.5a/\text{sec}$	57
B-1 Finite Element Model for the Area Between the Labrador Coast and Greenland	62
B-2 Distribution of Water Velocity Along Line $U-X$ for Different Positions of Pressure Centre	63
B-3 Distribution of Water Velocity at Line $U-V$ for Different Positions of Pressure Centre	64
B-4 Water Velocity at the Centre of the Area VS. Position of Pressure Centre	65
B-5 Location of the Study Area	66
B-6 Depth Profile for the Studied Area Between Greenland and Labrador Coast	67
B-7 Water Velocity at Ocean Current Area Near Saglik VS. Position of Pressure Centre	68
B-8 Water Velocity at the Middle of the Ocean VS. Position of Pressure Centre	69

CHAPTER I

INTRODUCTION

Iceberg motion has been of interest to various groups for many years. This has been due primarily to the need for monitoring iceberg movements near shipping routes, offshore drilling platforms and buried pipelines or cables. Icebergs weighing up to ten million tons may present a threat to the development of oil exploration by disrupting or destroying offshore structures or scouring bottom buried pipelines or cables.

In spite of the serious problems they cause to the offshore petroleum industry, icebergs present a potential solution to water supply problems in a number of dry areas of the world such as the deserts of Australia, Chile and Saudi Arabia. In view of the fact that 85 per cent of the world's available freshwater resides as ice in the Antarctic and Greenland (Weeks and Campbell, 1973), the interest is presently increasing in the utilization of icebergs as a source of freshwater and other secondary applications (e.g. cold utilization).

1.1 Background

Icebergs of the Southern Hemisphere are produced by ice shelves of the Antarctic. These icebergs are mainly of tabular shapes and can be as long as 170 km. Due to their size and shape they are stable and can survive in cold water for many years.

Icebergs of the Northern Hemisphere are produced from the glaciers of Greenland, the Northeastern Canadian Arctic, Spitsbergen, the Siberian Islands and Southeastern Alaska. The areas where icebergs are most fre-

quently encountered and where they interfere most with man's activities are in Baffin Bay, the Labrador Sea and the Grand Banks of Newfoundland. These icebergs are on the average much smaller than those of the Antarctic and have very erratic shapes. Icebergs seldom exceed a few kilometers in length and by the time they reach the southern Labrador Sea they are rarely longer than one kilometer. Of about 40,000 icebergs annually produced by Greenland glaciers, only an average of 380 cross the 48°N latitude (Murray, 1969). However during the 1972 season, a record of 1,587 icebergs were counted by Ice Patrol south of 48°N latitude. Most of the icebergs drift over a period of one to two years across Baffin Bay and through the Davis Straits into the Labrador Current. This current carries the icebergs southward to the Grand Banks of Newfoundland.

1.2 Iceberg Hazards to Offshore Operations

With the exception of human error, the iceberg probably poses the largest threat to Eastern Canada's offshore oil drilling and production operations. In view of the hydrocarbon potential in the Labrador Continental Shelf and the recent discovery of oil in the Grand Banks of Newfoundland, the need has risen for year-round operations and, hence, effective protection from icebergs. Small and medium icebergs are towed away while the big ones can be avoided by moving the platform. Dynamically stationed drilling vessels can evade icebergs by fast disconnect procedures and subsea acoustic re-entries. Both strategies require a method to identify a dangerous iceberg with sufficient lead time to adopt a defensive action. Dempster (1979) suggested an operational procedure to be followed by rig operators to avoid iceberg collision using a hybrid dynamic/kinematic

prediction model.

An accurate model to predict iceberg drift will reduce the risk of collision and the time and cost of unnecessary towing of icebergs or removal of the drilling vessel.

1.3 Statement of the Problem

The purpose of this study is to develop an accurate and easy-to-handle model that can be used on the deck of a drilling vessel to predict the drift of icebergs.

A mathematical model to predict the iceberg drift trajectory has a few parameters which depend on the characteristics of icebergs (e.g. mass, area under and above water, drag coefficients in water and air), and the predicted iceberg trajectory of such a model depends largely upon the input to the model which are the environmental forces (e.g. wind and current velocities). The validity of such a model is based on the comparison of the predicted trajectory with the observed trajectory of an iceberg under any conceivable combination of forces. For this purpose, attention will be paid to the iceberg trajectories which were recorded near Saglek, Labrador, by the Faculty of Engineering, Memorial University of Newfoundland, in August of 1972 during which time a low pressure system passed over the area causing deviations from the regular iceberg tracks (Figs. 1-1 and 1-2).

Though detailed data on iceberg drift trajectories and wind velocity is available, there is limited information about the parameters of the icebergs and the current velocity near the icebergs under investigations. Under these circumstances, detailed analysis

4

is carried out on iceberg trajectories where detailed information about current data is available and an effort is made to estimate iceberg parameters using information published in the literature.

Finally the results are compared to the observed trajectories to check the validity of the model.

1.4 Thesis Outline

Chapter 1 is an introduction.

Chapter 2 presents the review of previous field, theoretical and experimental studies on iceberg drift.

Chapter 3 describes the mathematical model and the selection of the input parameters to the model.

In chapter 4 a detailed study is presented on an observed iceberg drift trajectory (#20C, Fig. 1-2) with an irregular U-turn that took place during a storm. A parametric study on an iceberg drifting in a steady geostrophic current is presented in non-dimensional coordinates.

Chapter 5 presents analysis of the observed trajectories, discussion of the results and concluding remarks.

Analog computer simulation techniques as well as some practical applications including looping and spiral motion of icebergs are presented in Appendix A.

A finite element study on the effect of changes in ocean surface elevation which are caused by low atmospheric pressure systems on the ocean current is presented in Appendix B.

CHAPTER II

REVIEW OF LITERATURE

2.1 Field Studies

Smith (1931) presented general drift patterns of iceberg motion under the influence of ocean currents and wind generated currents based on iceberg observation near the Grand Banks. Post (1956) has shown that the drift of icebergs in the North Atlantic is mainly due to the relative strengths of the Labrador current and the Gulf stream. Kollmeyer (1969), Bruneau and Dempster (1971), and Dempster and Bruneau (1973), indicated that water currents are the primary driving force. Icebergs with large draughts are found to be influenced strongly by deep steady currents while small bergs are more sensitive to wind-induced surface currents. The direct wind force on the above water portion of the iceberg is considered to be significant if the wind speed is greater than fifteen knots (7.72 m/sec) and its direction is constant for periods of the order of days.

Dempster (1974), carried out field observations on eighty icebergs and ocean currents near Saglek, Labrador, in 1972. The study indicates that the main influence on iceberg motions is the strong Labrador current, the semi-diurnal current, a secondary current resulting from a bottom effect, and, for a brief period, inertial currents resulting from the effects of a severe storm.

Russell (1973) presented field measurements of the current off the coast of Newfoundland which were found to be rotary with periods of 15.5 hrs., almost equal to the theoretical period of inertial currents. The study of measured iceberg tracks indicated that the loops made by icebergs

could be caused by inertial current effects.

Soulis (1976) studied the cross-correlation of the iceberg drift with the wind and current forces using a kinematic model to approximate the dynamic equations of motion by assuming that the iceberg velocity would be the sum of the mean current velocity and some transformation of the transitory component of the current. The study indicated that the iceberg moved 2.5 times faster than the current at depth of 13 meters.

Russell, Riggs and Robe (1977) reported on a field study on two icebergs, and on a laboratory model. In the field study two icebergs were tracked for a number of days while drogues were used to measure the currents in the vicinity. The relative drifts between the icebergs and two drogues (one near the surface and the other at a depth of 100 m) were recorded. The analysis of the results indicated that the iceberg moved more closely to the deep drogue and that no simple correlation with the local wind field was found.

Ettle (1974), reported on a field observation by the U.S. Coast Guard on eight icebergs in the period of 1965-1968. It was found that at low wind speeds the effects of permanent currents, older wind-driven currents, and tidal currents predominate over wind drag and new wind-driven currents, whereas at wind speed of over ten knots the wind has a significant effect on the drift of an iceberg. The ratio of the drag coefficient for the iceberg's above water portion to the drag coefficient for its submerged portion was found to range from 1.5 for strong winds to approximately 7 for weak winds.

Riggs, Babu, Sullivan and Russell (1979) reported on a field study

7

carried out in the summer of 1978 where four hundred icebergs were tracked by a radar station for periods of up to 275 hours. Iceberg size and shape as well as current measurement were obtained. A general relationship between the current pattern and the iceberg tracks was observed. Some iceberg tracks, however, exhibited significant looping and curving during and after the passage of low pressure systems through the area. The gyrations and periods of these loops were much larger than those reported by Dempster (1974) and Russell (1973).

Robe, Maier and Russell (1979) presented a study on five icebergs tracked by the NIMBUS-6 satellite for periods from 138 to 202 days. The icebergs observed along the Baffin Island Coast were aground from 8% to 73% of the time. Maximum daily average speeds were found to be about 0.6 m/sec. The drifts were found to be generally coastwise in a southerly direction.

2.2 Theoretical Studies

Schell (1962) estimated the drifts of icebergs due to ocean currents and wind-generated currents and indicated that wind has a significant effect on the drift of the iceberg if it continues in one direction over a long period.

Murray (1969), discussed the factors that affect the drifts of icebergs and pointed out the efficiency of the statistical approach in the determination of their drifts.

Cochkanoff, Graham and Warner (1971) studied iceberg motion under the effect of water currents and Coriolis force. An analog computer model was used to solve the differential equations of motion. In the mathematical

model, the damping force was assumed to be proportional to the square of relative velocity of water current with respect to the iceberg. The results indicated that for large Coriolis forces relative to drag and inertia forces, the motion becomes more oscillatory before approaching the current direction.

Sodhi and Dempster (1975) presented the response of icebergs due to changes in velocity of water. The equations of motion were derived by assuming that the water drag force is proportional to square of relative velocity of the water with respect to the icebergs and assuming that icebergs respond mainly to currents, thus neglecting the effect of Coriolis forces. Exact solutions were obtained for two cases - rotary tidal currents and sudden change of translatory current velocity.

Cheema and Ahuja (1978) used a kinematic model to analyze the available data on iceberg drift in the Grand Banks. In this model the velocity of iceberg is assumed to be directly proportional to current velocity. Based on the study, suggestions have been made to improve the future data collection activities.

Mountaif (1979), has developed a numerical model to predict iceberg drift. A fourth order Runge-Kutta technique was used to integrate the equations of motion which consider iceberg acceleration, the water drag, the air drag, the Coriolis acceleration and a sea surface slope term. Testing of the model over long periods of time using observed drifts of icebergs suggests that model error is somewhat random in nature and probably originated from inaccuracies in the current and wind information supplied to the model.

Napoleoni (1979) presented several numerical dynamic models for prediction of iceberg drift. In addition to the environmental loading, iceberg rotation and acceleration of water are taken into consideration for the drift trajectory prediction. The results indicated that iceberg rotation can dramatically alter the drift and that Coriolis force has significant effects on iceberg drift.

2.3 Experimental Work

Russell, Riggs and Robe (1977) described a laboratory model designed to study motions of spherical and cubical semi-immersed objects made of paraffin wax whose specific gravity was roughly the same as that of icebergs. Experiments were performed with roughened models with a trip wire attached to ensure turbulent flow in the boundary layer. The results of this study and the field study described above indicated that the values of steady-state drag coefficient, C_D , determined in the model study were lower than values normally quoted for iceberg motion. This is due to the inclusion of the inertial term in the drag force equation. It was pointed out that the practice of ignoring the inertial drag term and incorporating the inertial coefficient into the steady-state coefficient may lead to erroneous drag force calculations.

CHAPTER III

ICEBERG DRIFT MODEL

3.1 Mathematical Model

Iceberg motion is the net result of a wide spectrum of forces which vary with time and space. Some of these forces are due to gravity, pressure gradient, wind drag, water drag, Coriolis effects, waves and swells. Since this study is mainly concerned with the horizontal movement of icebergs, only the horizontal components of these forces need to be considered. Wave and swell forces are generally neglected as their magnitude is small in comparison to other forces in the horizontal directions. The mathematical model, described in the present study, takes into account the significant environmental forces due to water drag, wind drag, Coriolis acceleration and sea surface slope (pressure gradient).

The drag force due to the water drag is proportional to the square of the relative velocity of water with respect to the iceberg. The constant of proportionality depends upon the size and shape of the under-water portion of the iceberg. The current is made of many components, a few of which are the geostrophic current, the wind-driven current, inertia current and tidal current. The distribution of the magnitude and direction of the various current components varies with depth. Hence, the ocean is considered in several layers, and the water drag force is then obtained as the vectorial sum of the drag forces in terms of relative velocity of current with respect to the iceberg in each layer.

The magnitude and direction of the wind drag force depend on the size and shape of the above water portion of the iceberg. The average ratio of

the iceberg velocity to wind speed is about 0.03 (Murray, 1969), so that the relative velocity of wind with respect to iceberg is taken to be the wind velocity itself in the expression for wind drag force.

The Coriolis force, caused due to the rotating frame of reference with the Earth, tends to move the iceberg and the water surrounding the iceberg to the right of their path (clockwise) in the Northern Hemisphere. In a geostrophic current, the pressure gradient force due to a sloping sea surface balances the Coriolis force due to its movement. If the iceberg motion is not along a geostrophic current direction, there are two forces acting on the iceberg: the Coriolis force due to its movement and the pressure gradient due to the sea surface slope. In the present study, the pressure gradient force in each layer will be expressed as the negative of the current's Coriolis force (Mountain, 1979) which is equivalent to expressing the Coriolis force on the iceberg in terms of the relative velocity of the iceberg with respect to the current in a particular layer.

If the water around the iceberg is accelerating due to some forces, the same forces would also be acting on the iceberg to accelerate the iceberg. So the force balance term must include a term which takes into account the force accelerating the water mass and the iceberg at the same time, and this force on the iceberg will be equal to the product of mass of iceberg and acceleration of water surrounding the iceberg (Bayly, 1971 and Napoleoni, 1979).

The equation of motion taking all the above mentioned forces into account is written below in the component form:

$$\frac{du}{dt} = \frac{1}{M} \left[\sum_{j=1}^n \left(\frac{1}{2} C_{Dw} \rho_w A_j (U_j - u) S_j + M_j \alpha_j \right. \right. \\ \left. \left. + M_j f (v - V_j) \right) + \frac{1}{2} C_{Da} \rho_a A_a W^2 \cos \theta \right] \quad (3.1)$$

$$\frac{dv}{dt} = \frac{1}{M} \left[\sum_{j=1}^n \left(\frac{1}{2} C_{Dw} \rho_w A_j (V_j - v) S_j + M_j \beta_j \right. \right. \\ \left. \left. - M_j f (u - U_j) \right) + \frac{1}{2} C_{Da} \rho_a A_a W^2 \sin \theta \right] \quad (3.2)$$

$$\frac{dx}{dt} = u \quad (3.3)$$

$$\frac{dy}{dt} = v \quad (3.4)$$

where

- x, y = position of the iceberg (x and y axes are in the direction of east and north, respectively).
- u, v = components of the iceberg velocity in the x and y directions, respectively.
- U_j, V_j = components of the current velocity in the j th layer.
- t = time.
- M = mass of the iceberg and the added mass.
- M_j = mass of water displaced by the iceberg in the j th layer.
- C_{Dw}, C_{Da} = drag coefficient of the iceberg in water and air, respectively.
- ρ_w, ρ_a = density of water and air, respectively.
- A_j = cross-section area perpendicular to the current direc-

tion in the j th layer.

- A_a = cross-section area perpendicular to the wind direction of the above water portion of the iceberg.
- S_j = $\sqrt{(u_j - u)^2 + (v_j - v)^2}$, the relative speed of current with respect to iceberg in the j th layer.
- α_j, β_j = components of water acceleration in the j th layer.
- f = $2\Omega \sin\phi$, Coriolis parameter.
- Ω = angular velocity of Earth rotation.
- ϕ = latitude.
- w = wind speed.
- θ = direction of wind measured anti-clockwise from x axis.

If the parameters related to the iceberg are known, the above set of equations may be integrated provided the current and wind data are supplied as the forcing function (or input to the model) to obtain the response of the model in the form of the iceberg velocity and position. Since the set of differential equations are coupled and non-linear, it is expeditious to integrate them with the help of a digital computer or an analog computer, and both of these computers are used in the present study. The details of the analog simulation are given in Appendix A. The 4th order Runge-Kutta method is used to integrate the set of equation, 3.1-3.4, with the help of a digital computer (PDP 11/40) along with a plotting facility.

3.2 Parameters of the Icebergs Under Study

Since the mass, area and drag coefficients of the icebergs under study are not known, these values are chosen from the range of values quoted in literature, and this section describes the manner in which the parameters used in the present study are selected.

a) Drag Coefficients

It has been shown by Hoerner (1965) that the drag coefficients in water, C_{Dw} , and in air, C_{Da} , depend on the Reynolds number, R_e . The values of R_e for icebergs are of the order of 10^7 (International Ice Patrol, 1960). The studies reported by the International Ice Patrol indicated that the drag coefficients must be higher than 0.2 but not higher than 1.0 and that the drag coefficient ratio for in air to water lies between 1.0 to 1.5. Eittle (1974) found that this ratio ranges from 1.5 for strong winds to about 7 for weak winds. In a study on iceberg towing Chirivella and Miller (1978) found out that R_e for in water is about 9×10^8 and for in air ranges from 10^7 to 10^9 and the corresponding values of C_{Dw} and C_{Da} are 1.0 and 0.9 respectively. Banks and Smith (1974) towed small icebergs on the Labrador Coast and obtained 1.2 as a mean value for C_{Dw} with a standard deviation of 0.2. Similar studies carried out by Weeks and Campbell (1973) on large icebergs indicated values of 0.6 to 0.9. In another iceberg towing experiment, Dempster (1979) found that a value of C_{Dw} taken as 0.5 to 0.7 produce the correct trends of motion but a value of 2.0 achieved the best fit between the computed and actual data. The high value of C_{Dw} , in his opinion is probably a composite of a drag coefficient and a correction factor to compensate for errors in the estimation of the system parameters.

Russell et al (1977) indicated that values of C_{Dw} that must be used in prediction of iceberg drift are usually very high because steady-state conditions are assumed. Such steady-state conditions are impossible to take place unless there is no relative motion between the iceberg and the water in which case the drag force is zero. Instead, the iceberg must accelerate and decelerate continuously. They concluded that the practice of ignoring

the inertial drag term and incorporating the inertial coefficient into the steady-state coefficient may lead to erroneous drag force calculations.

It can be concluded that water drag coefficient for iceberg calculations ranges between 0.6 to 1.2 and that the ratio C_{Da} / C_{Dw} is somewhere around 1.5.

It has been decided to use a value of C_{Dw} of 1.0 and C_{Da} of 1.5 regardless of the size and shape of the iceberg.

b) Added Water Mass

The concept of "added water mass" is introduced to account for inertial drag. Inertial drag arises because of the acceleration of the fluid around the object. The object behaves as if a mass were added to it. The added water mass can be determined from the potential flow theory.

The added mass in our model is assumed to be half the mass of iceberg which agrees with measurements made by Hamilton and Lindell (1971) and calculations made by Lamb (1879) for spherical and cubic objects.

c) Iceberg Mass and Cross-Sectional Area

Iceberg parameters needed for the model are the mass and the cross-sectional area in each water layer and in the air (Eqn. 3.1). This information cannot be obtained operationally for each iceberg. Instead observations made over a number of years have been used to establish seven classes of icebergs which could be distinguished from aircraft. Table 1 presents the average areal and mass characteristics for each class as published by Mountain (1979). Iceberg parameters needed for this study are chosen from this table.

CHAPTER IV

RESULTS

4.1 Introduction

In the first part of this chapter, a parametric study of the iceberg drift model is presented in which the trajectory is obtained for an iceberg drift in a steady current starting from rest. This study shows the dependence of the iceberg trajectory on the parameters obtained by writing the equations of motion in a non-dimensional form.

In the second part of this chapter, the verification of the iceberg drift model, presented in the previous chapter, is attempted by comparing the trajectories predicted by the model with that of iceberg #20C observed near Saglek, Labrador, in 1972. The data used as input to the model are the current and wind data obtained in the field. The comparison between the predicted and observed iceberg trajectories is good.

4.2 Drift of an Iceberg Starting from Rest in a Uniform Current

Iceberg grounding is a frequent occurrence, and in fact icebergs have been observed to remain grounded for the 40% of the observation time (Robe, Maier and Russell, 1979). The icebergs sometimes become loose and start drifting again which provides the motivation of this study. The trajectory of an iceberg under the influence of only a uniform and steady geostrophic current in the x-direction, U, is governed by the following equations of motion which are obtained from equations 3.1 and 3.4 assuming the water column to have a constant velocity at all depths.

$$\frac{du}{dt} = \kappa(U-u) \sqrt{(U-u)^2 + v^2} + fv \quad (4.1)$$

$$\frac{dv}{dt} = -\kappa v \sqrt{(u-u')^2 + v'^2} - f(u-u') \quad (4.2)$$

$$\frac{dx}{dt} = u \quad (4.3)$$

$$\frac{dy}{dt} = v \quad (4.4)$$

where

$$\kappa = \frac{C_{Dw} \rho_w A}{2M}$$

the initial values of x , y , u and v are assumed to be zero at the beginning of the integration process. The above set of equations can be written in a non-dimensional form as given below:

$$\frac{du'}{dt'} = (1-u') \sqrt{(1-u')^2 + v'^2} + \tau f v' \quad (4.5)$$

$$\frac{dv'}{dt'} = -v' \sqrt{(1-u')^2 + v'^2} + \tau f (1-u') \quad (4.6)$$

$$\frac{dx'}{dt'} = u' \quad (4.7)$$

$$\frac{dy'}{dt'} = v' \quad (4.8)$$

where $t = 1/U\kappa$, $u' = u/U$, $v' = v/U$, $t' = t/\tau$, $x' = x\kappa$ and $y' = y\kappa$.

The positions of the iceberg (x' , y') are plotted for various values of τf in Fig. 4-1. The positions of the icebergs are marked after intervals of $t' = 2$. The parameter τf takes into consideration the Coriolis factor and the iceberg characteristics such as mass, area under water, density and drag coefficient. The range of values assumed for τf have been computed from the values given in Table T for area and mass of icebergs.

These plots are similar to those obtained by Cochkanoff, et al (1971) using analog simulation of the problem. The initial motion is the resultant of the forces due to the water drag, and the pressure gradient (the sea

surface slope) caused by the geostrophic current. As the iceberg picks up speed, the drag force decreases, and the Coriolis force increases to counterbalance the pressure gradient force. The initial wavy motion of an iceberg as depicted by curve 5 in Fig. 4-1 is the result of interaction of the pressure gradient force and the Coriolis force. After a long time from the start of the iceberg motion, the trajectories become straight in a steady-state drift.

4.3 Study of an Iceberg Trajectory Near Saglek

In August of 1972, the Faculty of Engineering and Applied Science of Memorial University of Newfoundland conducted an oceanographic investigation collecting data on iceberg drift, currents and winds. A full account of their activities has been described by Allen (1972). Icebergs were tracked using a radar installed in a shore station at Saglek, Labrador, while the C.S.S. "Dawson" provided by the Bedford Institute of Oceanography, together with the Canadian Armed Services, Maritime Command, collected oceanographical and meteorological data in the vicinity. A total of one hundred and ten icebergs were tracked, some for several days and others for only several hours. The scientific party aboard the "Dawson" obtained extensive data on currents at four locations as shown in Fig. 4-2. The current meters were installed at depths of 13m and 75m at each of these four locations, and three additional current meters were installed 10m above the sea bottom at locations A, B and C, shown in Fig. 4-2. The data obtained from the current meters is presented and analyzed by Holden (1974). His conclusions are that the current at Saglek oscillated with the tidal period of 12.5 hours before the storm of August 22, 1972, and the oscillation period after the storm was inertial for current meters

close to the surface of water. This suggests that the storm influenced the flow conditions in the oceanic boundary layer.

The iceberg drift trajectories obtained before, during and after the storm along with the current and wind data present a unique opportunity to test the iceberg drift model. The information related to the shape, mass and areas above and below water of the icebergs under investigation are not available, and reasonable values of these parameters have been assumed from the data quoted in the literature (Mountain, 1979).

In the following, we present the results of two studies based on this set of data and their main conclusions. Later, the discussion is continued with the results of the present study.

a) Soulis (1976) used the drift data of approximately 33 icebergs to determine a vector cross-correlation between the iceberg drift velocity and the wind and current data. Although detailed behaviour of an iceberg is highly individual, Soulis (1976) concluded that, in general, "the iceberg studied:

- 1) moved 2.5 times faster, but in the same direction as, the mean current experienced by the iceberg at a depth of 13 meters.
- 2) had a transitory velocity component which equalled 0.5 of the transitory current experienced by the iceberg at a depth of 13 meters and lagged 73° .
- 3) had a wind-induced velocity component equal to 4% of and 25 degrees to the right of, the wind velocity."

The above conclusions by Soulis (1976) have been arrived at by correlating the iceberg drift velocity with the current data obtained at 13

meters depth. These results should be used with care because an iceberg extends below the oceanic boundary layer which is about 30 to 40 m deep, and the current data on the 13 meter level would be an indicator of current composition in the boundary layer only. A similar cross-correlation between the iceberg velocity vectors and the wind and deeper current velocity was not attempted perhaps due to malfunctions of the two current meters at 75 meters below sea surface level. However, all the current meters 10 meter above sea bottom were operational and, perhaps, cross-correlations between the current data obtained from those current meters and the iceberg drift velocity may have been meaningful.

b) Dempster and Bruneau (1973) have given a general explanation that the icebergs move under the influence of currents which cause them to have trajectories in the form of loops and spirals when there is weak or no wind. As mentioned earlier, the storm which moved over the area on August 21-22, 1972, caused considerable disturbance in the trajectories of four icebergs. Dempster and Bruneau (1973) suggested an explanation for these deviations to be the effect of currents set up due to changes in the sea surface elevation as the low atmospheric pressure zone passed over the area. For a motionless sea and homogeneous water, the change in height (h) of the sea surface is related to the change in the atmospheric pressure (P_a) by the expression (Neumann and Pierson, 1966).

$$\Delta h(\text{cms}) = -\Delta P_a \quad (\text{mbars}) \quad (4.9)$$

The above expression shows that in the areas of low atmospheric pressure the sea surface level must be higher than the mean sea level, and vice versa. Although the inverse pressure law is not strictly applicable to a dynamic, non-homogeneous ocean, it does give an indication of magnitude.

of disturbance caused by an atmospheric pressure.

When the sea surface level changes, the currents are set up to satisfy continuity, and the equation of continuity is written below (Neumann and Pierson, 1966):

$$\frac{\partial u}{\partial x} + \frac{\partial v}{\partial y} = \frac{1}{h} \frac{\partial \eta}{\partial t} \quad (4.10)$$

where u and v are the horizontal water velocities in the x and y directions, h the depth of ocean and $\eta(t)$ is the change of sea surface level above the mean level at a particular time t . During the storm, the atmospheric pressure fell by a total of 36 to 38 millibars in about 6 to 8 hours which would result in a very low rate of change in sea surface elevation $(\frac{\partial \eta}{\partial t})$. Further, the depth of ocean is in the order of 100m and more which makes the right hand side of equation 4.10 insignificant. A detailed finite element analysis was undertaken to solve equation 4.10 taking various ocean depths into consideration, and the results show that the currents developed due to changes in sea surface level are negligible when the ocean depth is in the order of 100 meters for the same approximate conditions as those prevailed during the storm. The details of this study are given in Appendix B.

c) Present Study

The only other reason for the complex iceberg trajectories during the storm can be the direct action of the wind on the sails of the icebergs and the indirect action of wind on the oceanic boundary layer resulting in wind driven currents which in turn affect the iceberg motion. Figure 4-3 shows the contours of atmospheric pressure system before and after the crossing of the storm centre through Sagiek, and it also shows

the reversal of wind directions during the storm. It is for this purpose the present study is undertaken to develop an iceberg drift model and compare the predicted iceberg trajectories to the observed ones. The sources of these data used to run the model are given below.

(1) Currents

As mentioned earlier, the current data is obtained from meters installed at four locations, A, B, C and D (shown in Fig. 4-2) and at three different levels below the sea surface level (A_1, B_1, C_1 and D_1 at 13m, A_2, B_2, C_2 and D_2 at 75m and A_3, B_3, C_3 10 meter above sea floor, which are 165m, 146m and 176m below the sea surface at locations A, B and C, respectively). The current meters A_2 and B_2 recorded only the current direction and not the magnitude due to some malfunction of this instrument. The data used for running the iceberg drift model uses the directions measured by A_2 and B_2 and the magnitudes measured by A_3 and B_3 . This is justified because the magnitude of the geostrophic current is approximately constant between the top and the bottom oceanic boundary layers.

Since the iceberg drift model considers the water column in two layers, the ocean boundary layer extending from the ocean surface to about 40 meters depth and the deeper layer from 40 meter depth to the ocean bottom, the current in the deeper layer is assumed to be geostrophic and constant with respect to depth for our calculations whereas the current in the boundary layer is assumed to be the vectorial sum of geostrophic and wind driven currents. Assuming that the structure of the wind driven currents to be in the form of an Ekman spiral, we can derive the information about the direction and magnitude of the water mass transport from the current meter data located in the boundary layer and in

deeper water.

If the wind shear stress vector is acting in the +y direction (i.e. to the north), the wind driven current velocity components to the east and north, u and v, are given by the following expression (Neumann, 1968).

$$\begin{aligned} u &= V_0 e^{-(\pi/D)Z} \cos(45^\circ - \pi Z/D) \\ v &= V_0 e^{-(\pi/D)Z} \sin(45^\circ - \pi Z/D) \end{aligned} \quad (4.11)$$

where $D = 36.7m/\sqrt{\sin\phi}$, V_0 represents the speed of the surface current, Z the depth below the water surface and ϕ the latitude of the location. The above current distribution is known as the "Ekman Spiral".

The latitude of Sagley is $58.5^\circ N$, and the depth of boundary layer $D=39.7$ meters which is approximately equal to the depth of mixing layer as is evident from the contour lines of the measured STD data (Allen, 1972). The net water mass transport, S_x and S_y in the easterly and northerly directions across 1 cm. width are given by (Neumann, 1968).

$$\begin{aligned} S_x &= \rho \frac{V_0 D}{\pi\sqrt{2}} \\ S_y &= 0 \end{aligned} \quad (4.12)$$

This is a remarkable result which states that total water mass transport is directed 90° to the right of the wind shear stress direction in the Northern Hemisphere and to the left of the wind shear stress vector direction in the Southern Hemisphere. The net effect of wind driven currents on the motion of an iceberg is to integrate the drag forces at different levels in the boundary layer. In this thesis, it is assumed that the boundary layer has a uniform velocity such that the net water mass trans-

port is equal to that given in equation 4.12 and the direction is 90° to the right of the wind shear stress vector. Thus, the average water velocity component in the boundary layer is $\bar{u} = 0.225V_0$ and $\bar{v} = 0$. Using equations 4.11, the velocity components at 13m below the sea surface level are:

$$u = 0.358 V_0 \cos(-13.9^\circ)$$

and

$$v = 0.358 V_0 \sin(-13.9^\circ)$$

Hence, we obtain a factor, equal to 0.628, which is the ratio of the magnitudes of the average velocity in the boundary layer to that at 13m level, and the difference between their directions is 13.9° .

The following procedure is followed to calculate the input data for the currents in the model described in Chapter 3 to predict the iceberg drift trajectories. Let the measured velocity components at the 75 meter depth be designated as U_g and V_g in the easterly and northerly directions, respectively, and let U_s and V_s be the designation given to the velocity data at 13 meter depth. The iceberg drift model needs the input current velocities at two layers of the water column U_1, V_1 in the boundary layer and U_2, V_2 in the deeper layer. For the deeper layer, the input velocity data is taken to be the same as the measured velocity, i.e. $U_2 = U_g$ and $V_2 = V_g$. The average water velocity components for the boundary layer are taken as follows:

$$\begin{aligned} U_1 &= 0.628[(U_s - U_g) \cos(13.9^\circ) - (V_s - V_g) \sin(13.9^\circ)] + U_g \\ V_1 &= 0.628[(U_s - U_g) \sin(13.9^\circ) + (V_s - V_g) \cos(13.9^\circ)] + V_g \end{aligned} \quad (4.13)$$

The equation 4.13 effectively performs the operations of adjustment of magnitude and direction on the vector of the wind generated current velocity and then adding the geostrophic components to obtain the average velocity in the boundary layer.

Since the current velocity vary spatially as well as temporally, the current data is interpolated from the currents values at corresponding depths at locations A and B to predict the trajectory of a particular iceberg designated as 20C whose drift path happened to be close to the current meters. A cubic interpolation function is used to give more weight to the current meter closer to the iceberg:

$$U_{\text{interpolated}} = U_A F + U_B (1-F)$$

$$\text{where } F = 3\xi^2 - 3\xi^3, \quad \xi = (Y_1 - Y_B)/(Y_A - Y_B)$$

U_A, U_B = data from current meters at A and B, respectively.

Y_1, Y_A, Y_B = ordinates of the iceberg position and locations A and B, respectively.

(ii) Wind Data

At first, the wind data was obtained from the atmospheric pressure charts obtained from Environment Canada (Gender office). The interpretation of these six hourly atmospheric pressure data was done by an experienced meteorologist (Mr. Duncan Finnyson of NORDCO Ltd., St. John's). The wind data thus obtained gave a good idea of the wind speed and directions.

As more detailed wind speed and direction at the sea surface are required to run the iceberg drift model, we obtained the wind data from the log books of C.S.S. "Dawson" where such data was recorded at 2 to 4

hours interval. A linear interpolation is used to deduce the wind speed and direction at an intermediate time.

4.4 Results

Since the mass and other parameters of the iceberg are not known, the trajectories of iceberg drift are obtained using small, medium and large non-tabular icebergs as given in Table 1, and Figs. 4-4 and 4-5 show the predicted trajectories along with the observed trajectory of iceberg #20C during the storm which passed over the area on August 21-22, 1972. The predicted trajectory of a medium non-tabular iceberg (Fig. 4-4) gives a good fit to the observed trajectory, and thus the iceberg #20C is assumed to be a medium non-tabular iceberg.

Fig. 4-6 shows two predicted iceberg trajectories when the iceberg is driven by the wind alone and by the currents alone. Fig. 4-7 shows two iceberg trajectories when the iceberg is driven by geostrophic currents only and by geostrophic currents and wind together. In these two figures, the effect of excluding a particular environmental force, can be seen as the observed iceberg trajectory is also shown there. It is evident from these results that currents and wind have significant effect on the iceberg drift.

Fig. 4-8 shows the effect of including and excluding the Coriolis force on the predicted iceberg drift trajectory. The Coriolis force must be included in the calculations for a good prediction of iceberg trajectory. Fig. 4-9 depicts the effect of including and excluding the water acceleration in the drift model. Though the net effect of excluding water acceleration term is not large, a better drift trajectory is obtain-

ed in this case by including the water acceleration term in the model.

Finally, Fig. 4-10 depicts two predicted iceberg drift trajectories when equation 4.13 is used to estimate the average water velocity in the boundary layer and when the current data at 13 meter depth is used as obtained (i.e., $U_1 = U_s$ and $V_1 = V_s$). As it is evident from the results, the current data at 13 meters depth alone does not give a good prediction of iceberg drift, and this data along with data at 75 meters depth has to be used to estimate the wind generated current in the boundary layer.

4.5 Discussion of Results

As mentioned earlier, one of the objectives of this investigation is to analyze the observed drift trajectories to find some interpretations of some of the observed strange behaviour of icebergs (looping, spiral motion and irregular U turns). A detailed study is presented in the previous section on the observed iceberg drift trajectory #20C with an irregular U-turn that took place during the storm. This study was feasible because the iceberg moved in the vicinity of two current meters (Fig. 4-2) and, hence detailed data on currents could be obtained. Unfortunately, no similar data is available for iceberg trajectories with loops. The looping motion either took place in locations far away from current meters (e.g., tracks #10F, 11L and 13G in Fig. 1-1, and 17B, 17D and 19B in Fig. 4-2) or close to a current meter but at a time where no current data is available (e.g. track #7M, Fig. 1-1). Therefore, detailed analyses, similar to that performed on trajectory #20C, can not be carried out for other trajectories. However, a better understanding of the looping motion can be obtained by studying the behaviour of iceberg under the same environmental conditions suggested to cause looping motion and other conditions under which icebergs

were reported to have spiral and looping motions. A detailed account of this study is presented in Appendix A, and the behaviour of icebergs during the storm that passed over Saglek on August 21-22, 1972 is discussed below.

Fig. 4-2 presents some of the iceberg trajectories that were disturbed by the storm. Generally speaking the icebergs moved back and forth forming either U-turns (#20C and 20D), or loops (#17B, 17D and 19B). The trajectories with U-turns were close to Saglek while the others were far to the north. This difference in iceberg behaviour seems to be due to difference in local current field. However, the direct action of the wind on the sails of the icebergs is evident from the fact that icebergs moved back and forth as the wind direction changed due to the passage of the storm centre through the area (Fig. 4-3), and that the deviation from the regular drift trajectories start and stop at about the same time (Fig. 4-2).

Availability of detailed current and wind data for iceberg #20C presented a unique opportunity to verify the validity of our model and to evaluate the significance of each of the forces included in the model (air drag, water drag, water acceleration and Coriolis force). The predicted drift trajectory of an iceberg is significantly influenced by the size of iceberg (Figs. 4-4 and 4-5). The assumption that iceberg #20C is a medium non-tabular iceberg is supported by visual observations made by Dempster (Personal Communication, 1980). The results presented in Figures 4-6 to 4-9 demonstrate the importance of each of these forces.

Due to the non-uniform distribution of the current velocity in the ocean boundary layer, the current data in the boundary layer along with data at deeper depths should be used to estimate the average velocity in the boundary layer for good prediction of the iceberg drift (Fig. 4-10).

CHAPTER V

CONCLUDING REMARKS

A dynamic model to predict iceberg drift has been developed and verified by comparing the predicted iceberg trajectory to that observed during a storm. Changes in ocean surface elevation due to a low atmospheric pressure system have no effect on ocean current in deep water depths as in the case near Saglek. The direct action of wind is the main cause of the observed back and forth motion of icebergs during the storm. The indirect effect of wind on the motion of icebergs is via wind-generated current and the changes in geostrophic current, if any.

Iceberg trajectories with loops and spiral motion were obtained under simulated conditions. However, no general conclusion to the cause of this behaviour can be drawn mainly because of the absence of the in-situ wind and current measurements for trajectories with such behaviour.

To our knowledge, this is the first published study where an iceberg drift model is tested during a storm using detailed current and wind data measured in the immediate vicinity of an iceberg. From this study it is evident that the physics of the iceberg drift model is known to extent that a good prediction of an iceberg trajectory during a storm can be made provided detailed current and wind data are available as input to the model.

It is recommended that a model to predict ocean currents is needed to generate the necessary data on currents which is to be input into the iceberg drift model. In the absence of such a model, the current data must be obtained by a string of current meters in the vicinity of a location where icebergs may be a threat to a particular installation.

TABLES AND FIGURES

Table 1. Iceberg Characteristics (Mountain, 1979)

Iceberg Type	Size	Mass (10^6 kg)	Dry Area (M^2)	Net Area (M^2) Per Depth Layer			
				0-20M	20-50M	50-100M	100-120M
NON TABULAR	Growler	.45	10	80	0	0	0
	Small	.75	230	780	870	0	0
	Medium	900	910	1800	1900	2700	0
	Large	5500	2000	3500	3750	5300	1400
TABULAR	Small	245	650	1900	2600	0	0
	Medium	2170	2700	4400	5900	8700	0
	Large	8235	5200	7200	9700	14,400	5,000

Table 2. Wind Data
 (From the Log Books of C.S.S. Dawson)

Date	GMT	Wind Speed (kts)	Wind Direction
August 20	0500	8	200
	0700	5	210
	1100	10	200
	1500	15	230
	1900	17	030
August 21	0300	10	240
	0500	9	150
	0700	9	150
	1100	15	120
	1500	25	135
	1800	30	125
	1900	27	125
	2100	20	320
	2300	20	320
August 22	0100	10	240
	0300	25	280
	0500	30	280
	0700	30	275
	0900	50	270
	1100	36	265
	1300	35	280
	1500	28	265
	1700	26	280
	1900	20	285
	2100	18	260
2300	18	260	

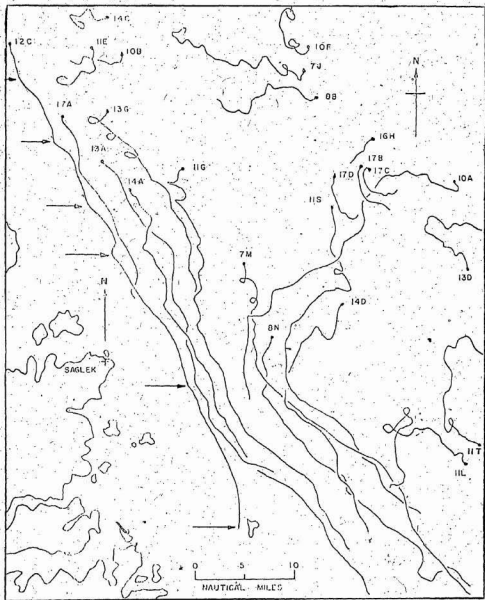


FIG. 1.1 DRIFT PATTERN OF ICEBERGS OFFSHORE SAGLEK BEFORE PRESSURE DISTURBANCE. (DEMPSTER AND BRUNEAU, 1973)

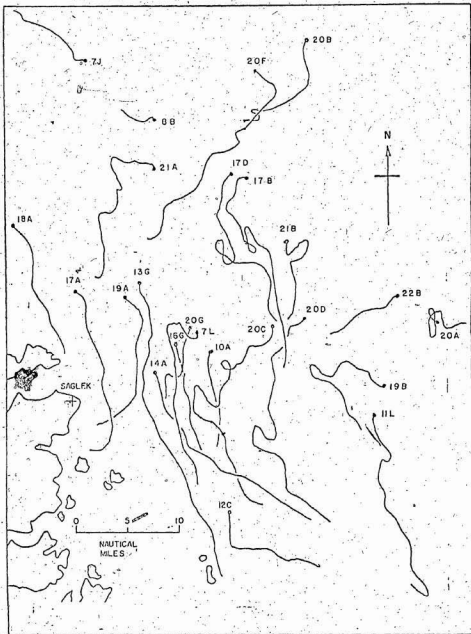


FIG. 1.2 DRIFT PATTERN OF ICEBERGS AFTER PRESSURE DISTURBANCE.
(DEMPSTER AND BRUINEAU, 1973)

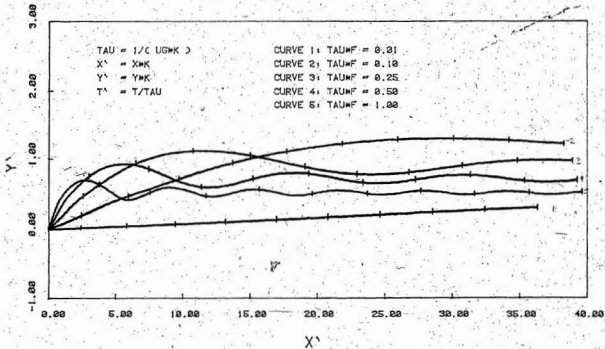


FIG. 4.1 DRIFT OF AN ICEBERG IN NON-DIMENSIONAL COORDINATES DUE TO GEOSTROPHIC CURRENT FOR DIFFERENT VALUES OF τu_{0F} . CURVES ARE MARKED AT EQUAL INTERVALS OF T' OF 2.

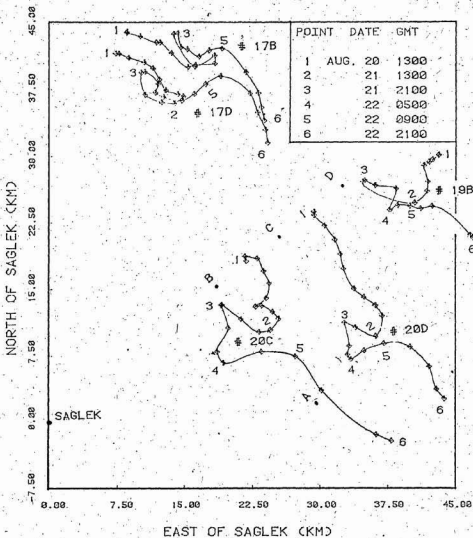
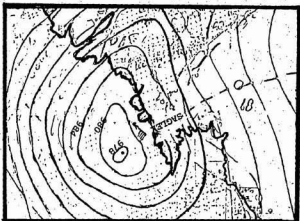


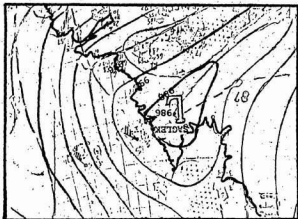
FIG. 4.2 DRIFT PATTERN OF ICEBERGS OFFSHORE SAGLEK AFTER THE STORM IN AUGUST 1972 SHOWING LOCATIONS OF CURRENT METERS.

FIG. 4.3 CONTOUR LINES OF ATMOSPHERIC PRESSURE
AS THE CENTER OF THE STORM PASSED THROUGH
SAGLEK.

AUGUST 22, 1972 - 0000 GMT.



AUGUST 21, 1972 - 1800 GMT.



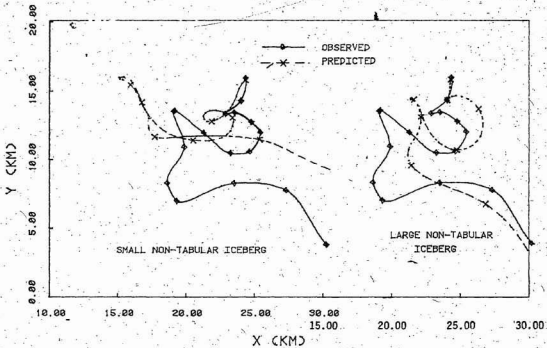


FIG. 4.5 EFFECT OF ICEBERG SIZE ON THE PREDICTED TRAJECTORY.

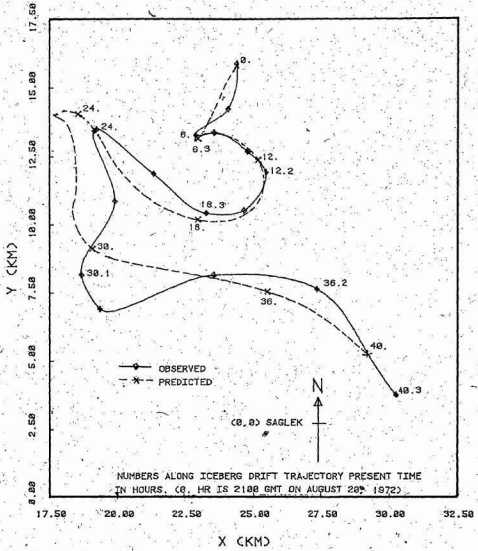


FIG. 4.4 PREDICTED AND OBSERVED TRAJECTORIES OF ICEBERG #20C DURING THE STORM WHICH PASSED OVER THE LABRADOR SEA ON AUGUST 21-22, 1972.

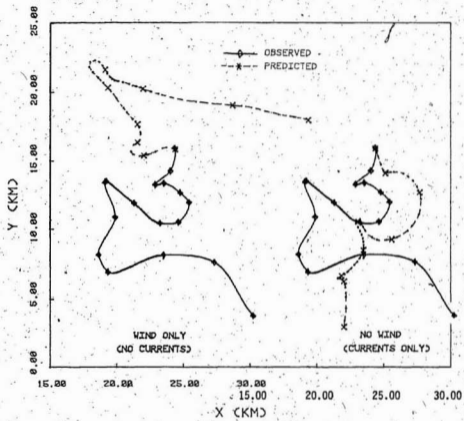


FIG. 4.6 EFFECT OF WIND FORCES ON ICEBERG DRIFT DURING STORM.

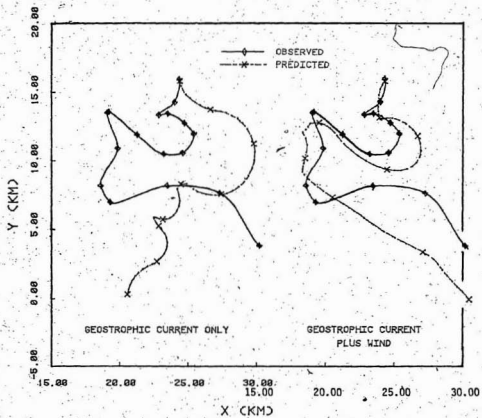


FIG. 4.7 ICEBERG DRIFT IN GEOSTROPHIC CURRENT WITH INCLUSION AND EXCLUSION OF WIND.

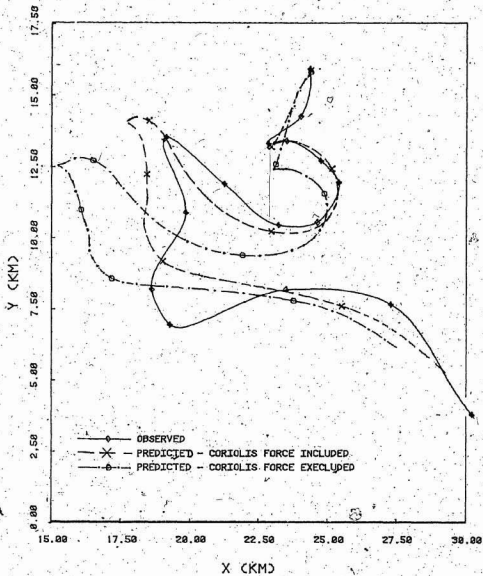


FIG. 4.8 EFFECT OF CORIOLIS FORCE ON ICEBERG DRIFT.

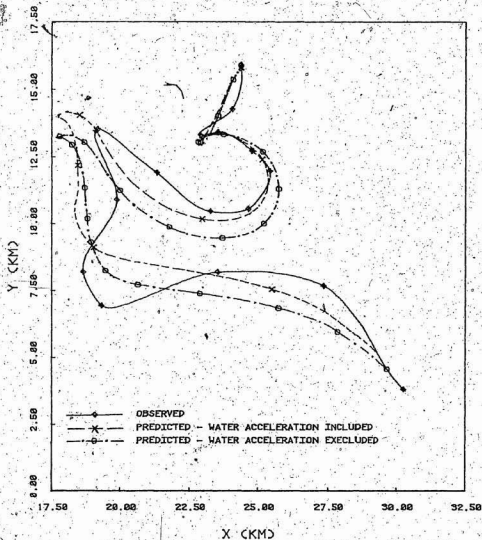


FIG. 4.9 PREDICTED ICEBERG DRIFT WITH INCLUSION AND EXCLUSION OF WATER ACCELERATION.

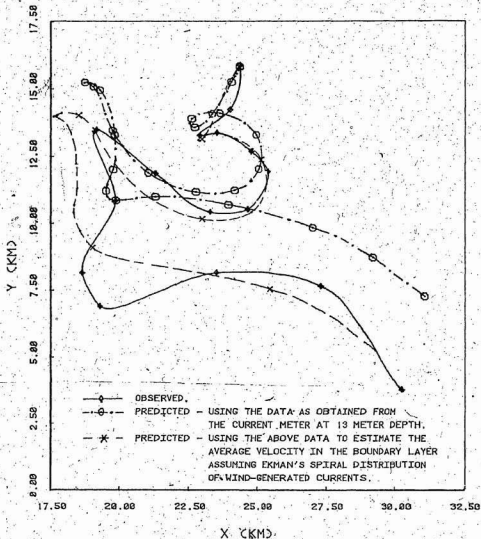


FIG. 4.10 EFFECT OF CONSIDERING THE DISTRIBUTION OF THE WIND-GENERATED CURRENT VELOCITY.

APPENDIX A

ANALOG COMPUTER SIMULATION

AND

SOME PRACTICAL APPLICATIONS

A.1 Introduction

One of the major benefits of analog processing is the ability to modify parameters during problem execution while observing its quantitative effects on a variable. In studying iceberg drift problems, this is particularly true when the program is being run in high-speed repetitive operation with the iceberg drift being graphically displayed. Typically, one can alter a coefficient value (e.g. iceberg parameter, current parameter, wind parameter, --- etc) while observing its effect on the iceberg drift. This technique presents a fast and efficient way to produce an iceberg drift trajectory similar to an observed track. This can be used to find an interpretation of the strange iceberg behaviour, e.g., looping after a storm. It can also be used to determine one of the model parameters (iceberg parameters, wind or current data) if the rest of the parameters and the iceberg track are known.

A.2 Techniques of Analog Computer Simulation

Problem solution by analog computers is accomplished by analogy, that is, the computer is programmed so that its circuit equations have the same mathematical form as the equations of the problem. In this type of computer, voltages represent various physical quantities, such as acceleration, force, displacement and so on. It is necessary, therefore, to arrange the voltages that present these variables and their

rates of change such that they will never have values larger than the voltage limitations of the computer (± 10 volts), nor such that they will ever change rapidly enough to exceed the frequency of the computer and its recording equipment. The generally accepted duration of a solution run is some where between 15 and 60 sec. (Jeness, 1965). If the solution takes too long, errors due to integrator drift will be introduced. On the other hand, if the solution time is too short, the permissible frequency limitations of the components and recording equipment may be exceeded. Keeping the maximum values of variables, their rate of change in the analog model, and the duration of the solution within the above-mentioned limitations is accomplished by "amplitude scaling" and "time scaling". The techniques of time and amplitude scaling described by Zulauf (1966), Rehoff (1967), and Hausner (1971) were used in scaling the analog variables.

To illustrate the analog simulation of the equation of motion and the scaling techniques, let us consider the case of an iceberg moving under geostrophic current. Considering the corresponding ocean surface slope and assuming no-wind condition, the equations of motion become:

$$\frac{du}{dt} = \kappa(U_g - u) \sqrt{(U_g - u)^2 + (V_g - v)^2} - f(V_g - v) \quad (\text{A.1})$$

$$\frac{dv}{dt} = \kappa(V_g - v) \sqrt{(U_g - u)^2 + (V_g - v)^2} + f(U_g - u) \quad (\text{A.2})$$

$$\text{where } \kappa = \frac{C_D \rho_w A}{2M} \quad (\text{A.3})$$

Time and amplitude scaling were chosen so that the length unit is 10 km

and time unit is one hour. This means that one second of the computer time represents a real time of one hour. A unit length in the model is equivalent to a real distance of 10 km. The length scale is 1 km/volt and velocity scale is (1 km/hr)/volt.

Having chosen these scales, then the requirements of the voltage and frequency limitations of the analog computer components are fulfilled. However, the maximum value of κ (Eqn. A.3) is approximately 24 which corresponds to a voltage of 240 (10 volt = unity). In order to keep the value less than unity (less than 10 volt), equations A.1 and A.2 can be rewritten as:

$$\frac{du}{dt} = \kappa' (5U_g - 5u) \sqrt{(5U_g - 5u)^2 + (5V_g - 5v)^2} - f' (5V_g - 5v) \quad (\text{A.4})$$

$$\frac{dv}{dt} = \kappa' (5V_g - 5v) \sqrt{(5U_g - 5u)^2 + (5V_g - 5v)^2} + f' (5U_g - 5u) \quad (\text{A.5})$$

where

$$\kappa' = \frac{\kappa}{25} \quad \text{always} < 1 \quad (\text{A.6})$$

$$f' = \frac{f}{5} \quad \text{always} < 1 \quad (\text{A.7})$$

So all the maximum values of the variables and coefficients in the analog model are kept below unity (less than 10 volt). The analog computer simulation of the above equations of motion is presented in Fig. A-1.

The programme circuit was patched on the patching panel of the computer. An oscilloscope and an x-y plotter were used to display and

plot iceberg drift and the time history of iceberg velocity.

A.3 Practical Applications

a) Effect of Coriolis and Pressure Gradient Forces

Some kinematic and dynamic models developed to predict iceberg drift ignore either Coriolis force or ocean slope (pressure gradient), or both. To estimate the error involved in such practice, iceberg drift in a geostrophic current is obtained for the different cases shown in Fig.

A-2. Coriolis force acts in $-y$ direction and the slope force in $+y$ direction. The results indicate that ignoring Coriolis force, ocean slope, or both leads to erroneous prediction of iceberg drift. The error is significant and increases as time increases.

b) Iceberg Drift in a Rotary Currents with Translatory Component

This kind of current has been observed and recorded by several investigators (Neumann, 1968). The iceberg trajectories are in the form of loops, the size of which and the distance between them are function of the ratio of the rotary to the translatory components. For large ratios, loops are large and close to each other. Fig. A-3 shows an example of iceberg drift under such conditions. Only one loop is shown in each case. Similar, but larger, loops in the iceberg drift have been observed by Riggs, et al (1979) in Lancaster Sound, Baffin Bay in summer of 1978.

c) Iceberg Drift in a Periodic Current

Fig. A-4 shows iceberg drift due to a horizontal current with velocity time history given by:

$$U_c = U_o \sin \omega t \quad (A.8)$$

The tidal movement of water in the Strait of Belle Isle has this type of velocity function. The iceberg moves in an elliptic loop the width of which is a function of the coefficient κ . Loop size is larger for large icebergs.

d) Inertial Motion of Iceberg

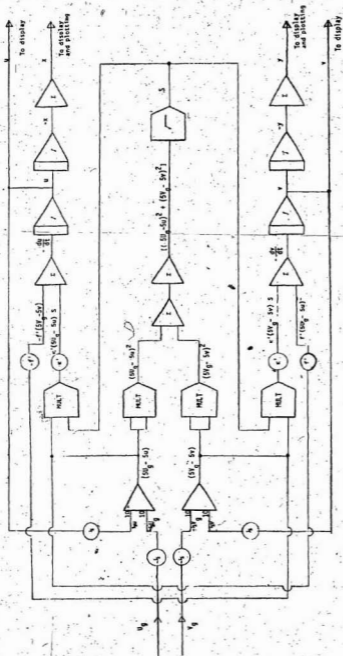
Fig. A-5 shows iceberg's motion after leaving a current field with an initial velocity u_0 . The family of curves show the effect of varying the initial velocity. For these cases it must be assumed that some aspect of the current or wind force has taken the iceberg from a major current into still water area. Under such conditions the iceberg moves in a spiral pattern and its velocity decays rapidly.

Fig. A-6 shows the iceberg trajectories of small, medium and large icebergs for a similar situation described above and for an initial velocity of 0.25 m/sec in each case.

e) Iceberg Motion in Currents Due to Inertial Oscillations

Fig. A-7 presents the drift of an iceberg with draught less than the depth of the oceanic boundary layer in a rotary current of 12 hrs.

If the iceberg has draught larger than the depth of the oceanic boundary layer, D , the iceberg will be affected by the drag force of the water below the oceanic boundary layer in addition to the rotary current in the boundary layer. If the water under the boundary layer is still, then the size of the loop is greatly reduced as seen in Fig. A-8.



Equations of motion:

$$\frac{dy}{dt} = v' (y_0 - 50) S - r' (y_0 - 50) + \frac{dy}{dt} = v' (y_0 - 50) S + r' (50 - y_0)$$

$$\text{where } S = \sqrt{(100 - y_0)^2 + (y_0 - 50)^2}$$

FIG. A-1 ANALOG COMPUTER SIMULATION OF ICEBERG MOTION - THE ONE LAYER MODEL

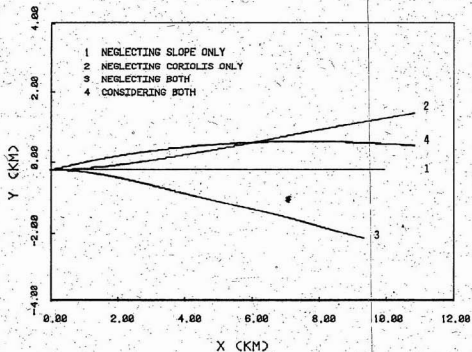


FIG. A-2 EFFECT OF CORIOLIS FORCE AND OCEAN SLOPE ON ICEBERG DRIFT DUE TO GEOSTROPHIC CURRENT OF 0.35 M/S

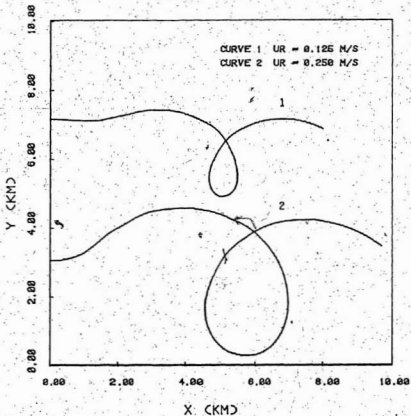


FIG. A-3 ICEBERG DRIFT DUE TO ROTARY CURRENT U_R PLUS A TRANSLATORY COMPONENT OF .085 M/S. PERIOD OF ROTARY CURRENT = 12. HRS.

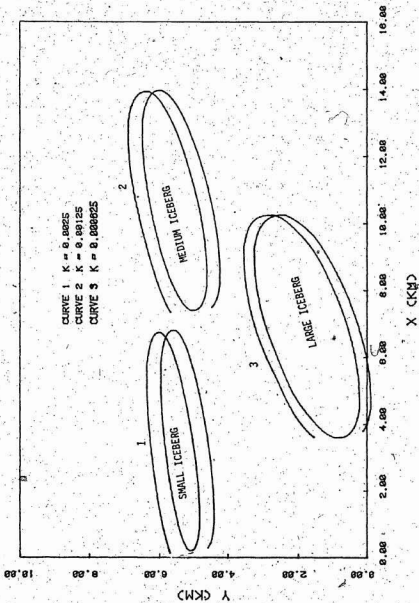


FIG. A-4 ICEBERG DRIFT FOR DIFFERENT VALUES OF K IN A HORIZONTAL CURRENT $U_C = U_0 \sin \text{CMT}$.

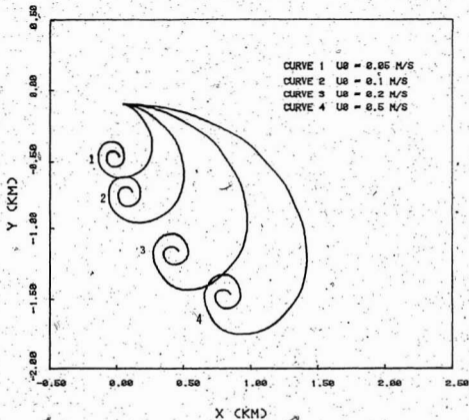


FIG. A-5 ICEBERG DRIFT UNDER CORIOLIS FORCE ONLY
 FOR DIFFERENT INITIAL VELOCITY U_0

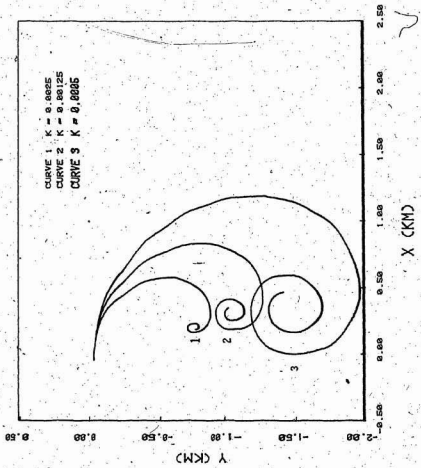


FIG. A-6 EFFECT OF K ON ICEBERG DRIFT UNDER CORIOLIS FORCE ONLY - INITIAL VELOCITY = 0.25 M/S

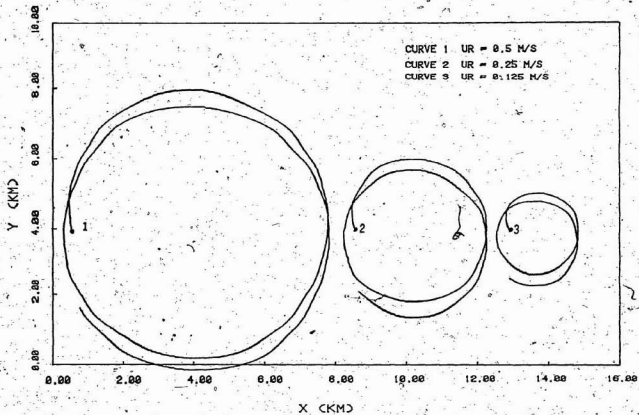


FIG. A-7 ICEBERG-DRIFT DUE TO INERTIAL CURRENT
 CURRENT PERIOD = 12. HRS

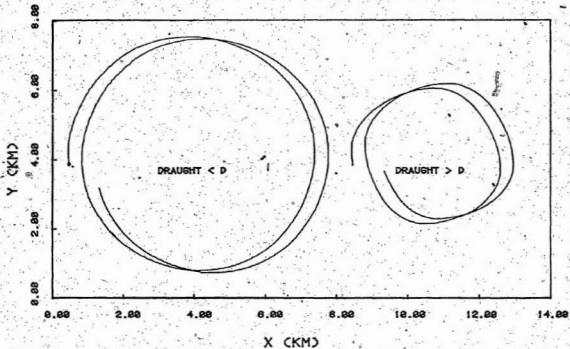


FIG. A-8 ICEBERG DRIFT DUE TO ROTARY CURRENT FOR TWO ICEBERGS WITH DRAUGHT LESS AND GREATER THAN THE DEPTH OF FRICTION LAYER D , $U_R = 0.5 \text{ M/S}$

APPENDIX B

EFFECT OF ATMOSPHERIC PRESSURE SYSTEM ON OCEAN CURRENTS INDUCED BY CHANGES IN SEA LEVEL

B.1 The Equation of Motion

The continuity equation for a body of water of constant depth h , with surface profile η (+ve downwards; Neumann and Pierson, 1966) is:

$$\frac{\partial u}{\partial x} + \frac{\partial v}{\partial y} = \frac{1}{(h-\eta)} \frac{\partial \eta}{\partial t} \quad (\text{B-1})$$

where:

u is the current velocity in x direction

v is the current velocity in y direction

The factor $(h-\eta)$ can be replaced by h since, usually, $\eta \ll h$, the Eqn.

B.1 can be written in the form:

$$\frac{\partial u}{\partial x} + \frac{\partial v}{\partial y} = \frac{1}{h} \frac{\partial \eta}{\partial t} \quad (\text{B.2})$$

For irrotational flow,

$$u = \frac{\partial \phi}{\partial x} \quad \text{and} \quad v = \frac{\partial \phi}{\partial y} \quad (\text{B.3})$$

where ϕ is the velocity potential.

Substituting from Eqn. B.3 into Eqn. B.2, we get:

$$\frac{\partial^2 \phi}{\partial x^2} + \frac{\partial^2 \phi}{\partial y^2} = \frac{1}{h} \frac{\partial \eta}{\partial t} \quad (\text{B.4})$$

or

$$\nabla^2 \phi = \frac{1}{h} \frac{\partial \eta}{\partial t} \quad (\text{B.5})$$

The boundary conditions of this problem may be prescribed by specifying the values of velocity potential, ϕ , and/or water velocities, u and v ($\frac{\partial \phi}{\partial x}$ and $\frac{\partial \phi}{\partial y}$), at the boundaries.

The finite element technique is used to solve the differential Eqn.

B.5.

B.2 Pressure Distribution

The moving low pressure system is approximated by a function similar to that of two dimensional normal (Gaussian) distribution defined by:

$$\eta(x, y, t) = P_0 e^{-\frac{1}{2}(x - C_x t)^2 / \sigma_x^2} e^{-\frac{1}{2}(y - C_y t)^2 / \sigma_y^2} \quad (\text{B.6})$$

where

η is ocean surface elevation (cm).

P_0 is the peak pressure (mbar).

σ_x and σ_y denote the extent of the pressure system in the x and y directions.

C_x and C_y are the components of the travelling speed of the system.

t is the time.

B.3 Practical Applications

a) Shallow Water

To study the effect of actual low pressure systems on ocean currents, the actual characteristics of the low pressure system that caused the storm over the North Atlantic in the period of August 21-22, 1972 have been used. That low pressure difference of 36 millibar which corresponds to a maximum rise of ocean surface of 36 cm. We assume the

atmospheric pressure distribution to be expressed by expression B.6 which gives reasonably similar pressure distribution to a low pressure system travelling at a fixed velocity.

The F.E. mesh of the 1600 x 1600 km area is presented in Fig. B-1. The centre of the pressure system was assumed to move along x-axis of the model, and the y-axis represents the Labrador Coast. The analysis starts from the moment the (edge of the) pressure system starts to enter the studied area. Since the effect of the pressure system is linear with respect to η/h values (Eqns. B.2 and B.6) it is decided to assume a water depth of 10m ($\eta/h = 0.036$). For other values of η/h , the results can be interpolated.

The results presented in Figs. B-2, B-3 and B-4 indicate that the maximum water velocity occurs under the centre of the pressure system (at the point of maximum surface elevation). Generally speaking, the water particles situated on x-axis moves in a direction parallel to the locus of the pressure centre. The water velocity at the centre depicts the back and forth movement of the waters.

b) Actual Case

The next step is to study the area of the ocean near Saglik, considering the actual profile of the ocean bed and an approximated pressure system (such as given by B.6). The minimum dimension of the F.E. model is taken to be about 1600 km as shown in Fig. B-5 between the Labrador Coast and Greenland. The F.E. discretization, the same as in Fig. B-1, and water depth profile is presented in Fig. B-6. Appropriate boundary conditions are used to simulate the shore at Labrador and Greenland (i.e. zero normal velocity to the shore line) and the open sea in the other two

sides of the F.E. model.

The results presented in Figs. B-7 and B-8 indicate that the effect of the low pressure system on water velocities is negligible due to the large water depth with respect to the peak pressure head. Also it is to be noted that the effect vanishes as the pressure system moves into areas with large water depths.

B.4 Discussion and Conclusion

When a low pressure system passes over an ocean, it raises the ocean surface and causes currents similar in nature to tidal currents. The current velocity is a function of size, traveling speed and the peak value of pressure system. It has been found that the effect of a low pressure system is significant in shallow water (e.g., for water depths less than 20m). Since ocean depth is about 100m in the area near Saglek, it has been found that the changes in current velocities due to the low pressure system is negligible.

The conclusion of this study is that the observed changes in iceberg paths during the storm were not necessarily due to the rise in ocean surface which was caused by the traveling low pressure system.

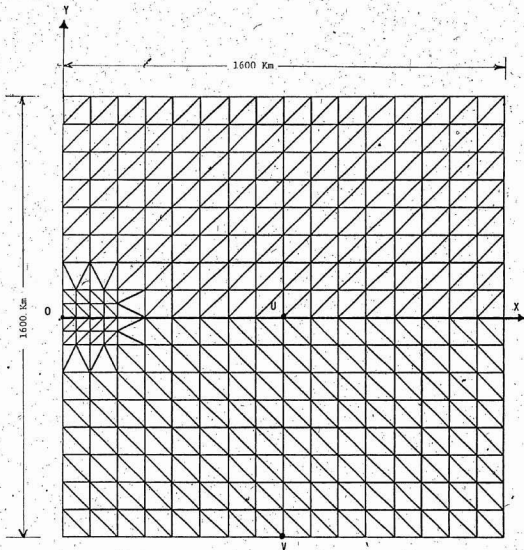


FIG. B-1 FINITE ELEMENT MODEL FOR THE AREA BETWEEN THE LABRADOR COAST AND GREENLAND

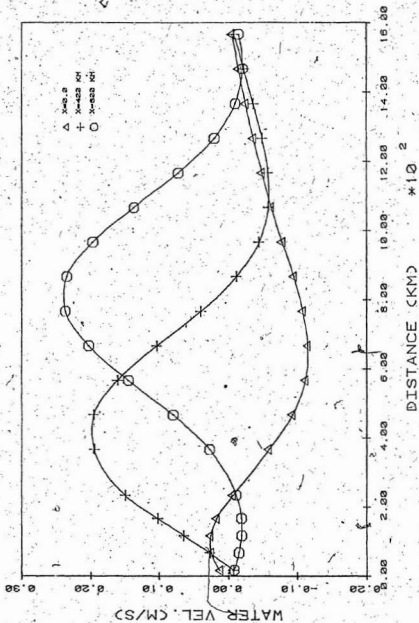


FIG. B-2 DISTRIBUTION OF WATER VEL. ALONG LINE 0-X FOR DIFFERENT POSITIONS OF PRESSURE CENTRE

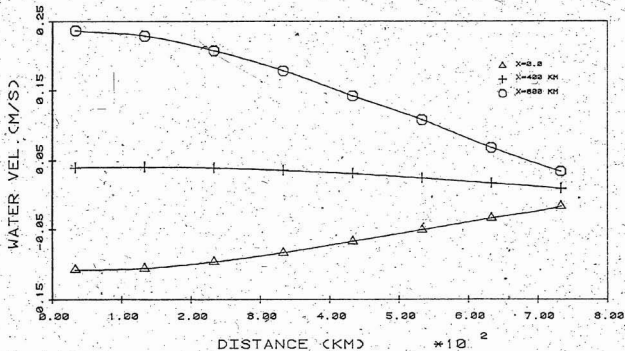


FIG. B-3 DISTRIBUTION OF WATER VEL. AT LINE U-V FOR DIFFERENT POSITIONS OF PRESSURE CENTRE

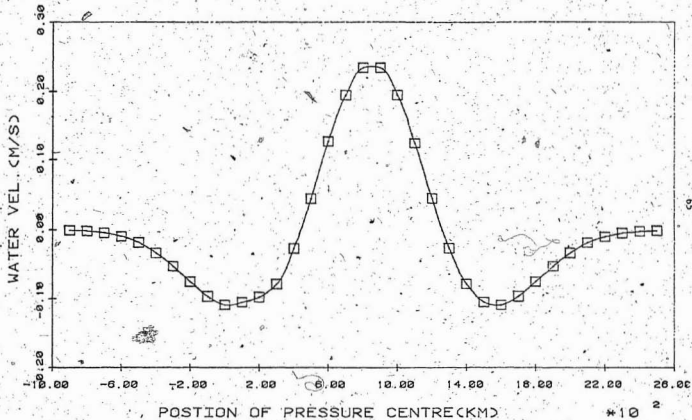


FIG. 8-4 WATER VEL: AT THE CENTRE OF THE AREA VS. POSITION OF PRESSURE CENTRE



FIG. B-5 LOCATION OF THE STUDY AREA.

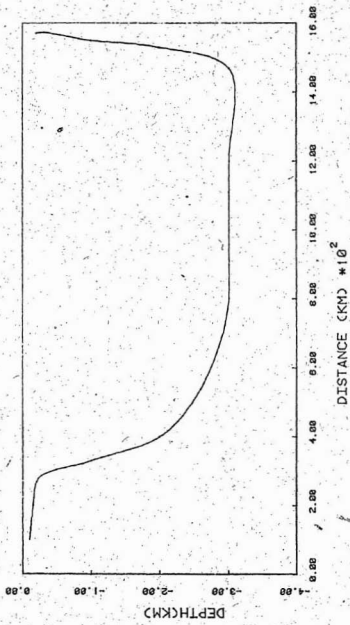


FIG. B-5 DEPTH PROFILE FOR THE STUDIED AREA BETWEEN GREENLAND AND LABRADOR-COAST

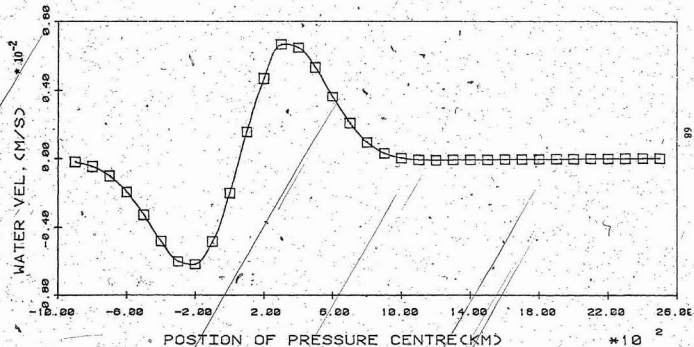


FIG. B-7 WATER VEL. AT OCEAN CURRENT AREA NEAR SAGLEK VS. POSITION OF PRESSURE CENTRE

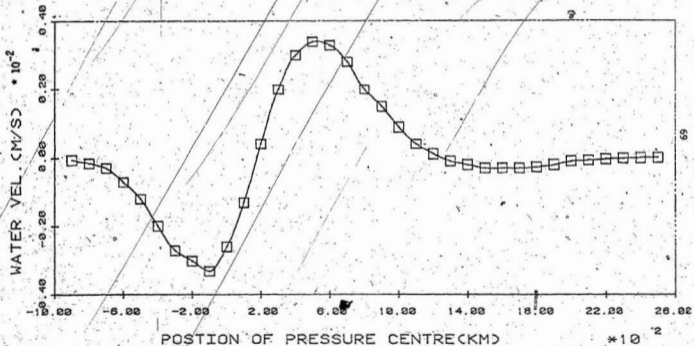


FIG. 8-8 WATER VEL. AT THE MIDDLE OF THE OCEAN VS. POSITION OF PRESSURE CENTRE

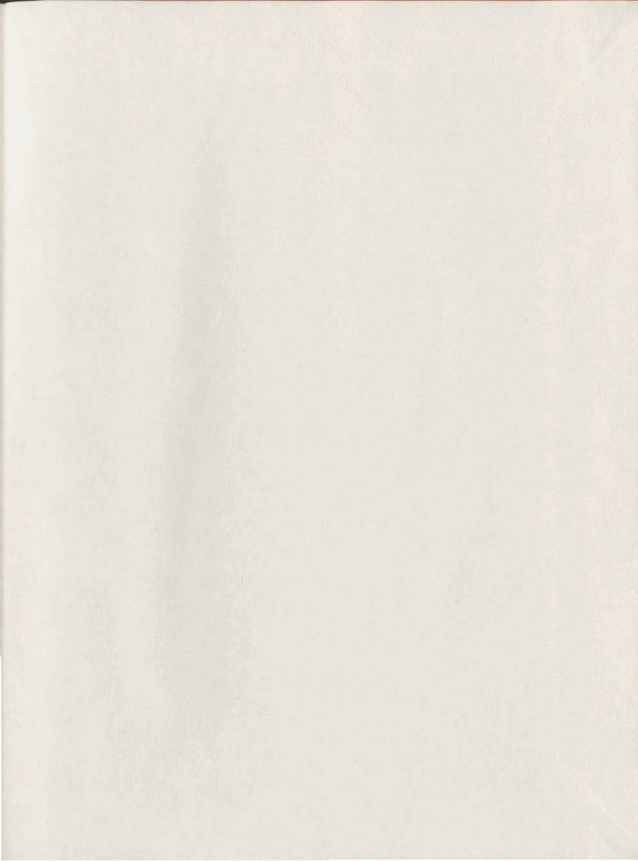
REFERENCES

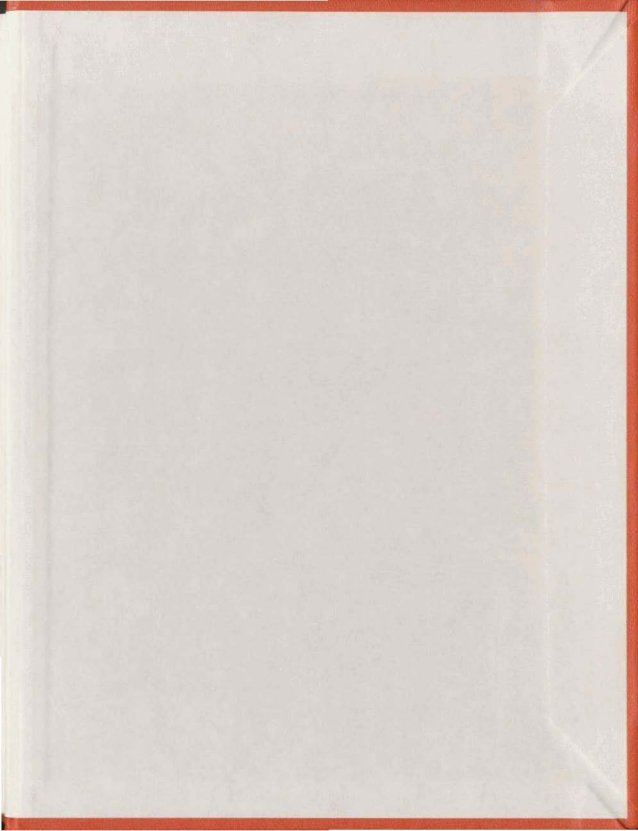
1. Allen, J.H., (1972), "Iceberg Study, Saglek, Labrador" including "Cruise Report C.S.S. Dawson, August 7 to August 26, 1972", Faculty of Engineering Report, Memorial University of Newfoundland.
2. Banke, E.G. and Smith, S.D. (1974), "Measurement of Towing Drag on Small Icebergs", IEEE International Conference on Engineering in the Ocean Environment, Halifax, Nova Scotia, August 21-23.
3. Bayly, I.M. (1971), "Contribution on the Inclusion of Certain Terms in the Equations Used in the Simulation for the Prediction of Ice Movement by Dr. O. Cochkanoff et al", Canadian Seminar on Icebergs, Halifax.
4. Bruneau, A.A. and Dempster, R.T. (1971), "Iceberg Dynamics", Report submitted to East Coast Petroleum Offshore Association.
5. Cheema, P.S. and Ahuja, H.N. (1978), "Drift of Iceberg in the Grand Banks", Ocean Engineering, Vol. 15.
6. Chirivella, J. and Miller, C (1978), "Hydrodynamics of Icebergs in Transit", Proc. First Int. Conf. on Iceberg Utilization, Ames, Iowa, U.S.A..
7. Cochkanoff, O.; Graham, J.J. and Warner, J.L. (1971), "Simulation Techniques in the Prediction of Iceberg Motion", Proc. Canadian Seminar on Icebergs, Halifax.
8. Dempster, R.T. (1979), "Characteristics of Iceberg Mechanics", IUTAM Symposium on Physics and Mechanics of Ice, Copenhagen, Aug. 6-10.
9. Dempster, R.T. (1974), "The Measurement and Modeling of Iceberg Drift", Proc. IEEE Conf. Ocean 1974, Halifax.
10. Dempster, R.T. and Bruneau, A.A. (1973), "Dangers Presented by Iceberg and Protection Against Them", Arctic Oil and Gas Conference, Le Havre, France, May 2-5.
11. Ertle, R. (1974), "Statistical Analysis of Observed Iceberg Drift", The Fifty-Third Annual Meeting of American Geophysical Union, Washington, D.C..
12. Hamilton, W.S. and Lindell, J.E. (1971), "Fluid Force Analysis and Accelerating Sphere Tests", ASCE, J. Hydraulics Division, June.
13. Hausner, A. (1971), "Analog and Analog/Hybrid Computer Programming", Prentice-Hall, Inc., Englewood Cliffs, N.J..
14. Hoerner, S.F. (1965), "Fluid-Dynamic Drag", Midland Park, New Jersey.
15. Holden, B.J. (1974), "Some Observations on the Labrador Current at

Saglek, Labrador", M. Eng. Project, Faculty of Engineering, Memorial University of Newfoundland.

16. International Ice Patrol (1960), "Wind Effect on Icebergs", Report of the United States Coast Guard.
17. Jenness, R.R. (1965), "Analog Computation and Simulation: Laboratory Approach", Allyn and Bacon, Inc., Boston.
18. Kollmeyer, R.C. (1969); O'Hagan, R.N. and Morse, R.M. (1969), U.S. Coast Guard Rep. No. 10.
19. Lamb, Sir Horace (1879) "Hydrodynamics", Dover Publications, New York, 6th edition, 1932, First published 1879.
20. Mountain, D. (1979), "On Predicting Iceberg Drift", The Iceberg Dynamic Symposium, St. John's, Newfoundland, June 4-5.
21. Murray, J.E. (1969), "The Drift, Deterioration and Distribution of Icebergs in the North Atlantic Ocean", Ice Seminar, Canadian Institute of Mining and Metallurgy.
22. Napoleoni, J.G.P. (1979), "The Dynamics of Iceberg Drift", M.Sc. Thesis, Dept. of Geophysics and Astronomy, Univ. of British Columbia, August.
23. Neumann, G (1968), "Ocean Currents", Elsevier Publishing Company.
24. Neumann and Pierson, W.J. (1966), "Principles of Physical Oceanography", Prentice-Hall.
25. Post, L.A. (1956), "The Role of Gulf Stream in the Prediction of Iceberg Distribution in the North Atlantic", Tellus, Vol. 8.
26. Rekoff, H.G. (1967), "Analog Computer Programming", Charles E. Merrill Books, Inc., Columbus, Ohio.
27. Riggs, N.; Babu, T.; Sullivan, M. and Russell, W.E. (1979), "Analysis of Iceberg Drift Patterns in Lancaster Sound", The Iceberg Dynamics Symposium, St. John's, Newfoundland, June 4-5.
28. Robe, R.Q.; Maier, D.C. and Russell, W.E. (1979), "Long-Term Drift of Icebergs in Baffin Bay and the Labrador Sea", The Iceberg Dynamics Symposium, St. John's, Newfoundland, June 4-5.
29. Russell, W.E.; Riggs, N.P. and Robe, R.Q. (1977), "Local Iceberg Motion - A Comparison of Field and Model Studies", POAC 77, Memorial University of Newfoundland.
30. Russell, W.E. (1973), "Current Studies in the Labrador Current With Respect to the Motion of Icebergs", M. Eng. Thesis, Faculty of Engineering and Applied Science, Memorial University of Newfoundland.

31. Schell, I. (1962), "On the Iceberg Severity of Newfoundland and Its Prediction", Journal of Glaciology, Vol. 4.
32. Smith, E.H. (1931), "The Marion Expedition to Davis Strait and Baffin Bay", Bulletin No. 19, U.S. Treasure Dept., Coast Guard, U.S. Printing Office, Washington.
33. Sodhi, D.S. and Dempster, R.T. (1975), "Motion of Icebergs due to Changes in Water Currents", IEEE Ocean 75.
34. Soulis, E.D. (1976), "Modelling of Iceberg Drift Using Wind and Current Measurements at a Fixed Station", M. Eng. Thesis, Faculty of Engineering and Applied Science, Memorial University of Newfoundland.
35. Weeks, W.F. and Campbell, W.J. (1973), "Towed Icebergs-Plausible or Pipe-dream?", J. Marine Technology Society, Vol. 7, No. 4, August.
36. Zulauf, E.C. and Burnett, J.R. (1966), "Introductory Analog Computation With Graphic Solutions", McGraw Hill Book Company, New York.







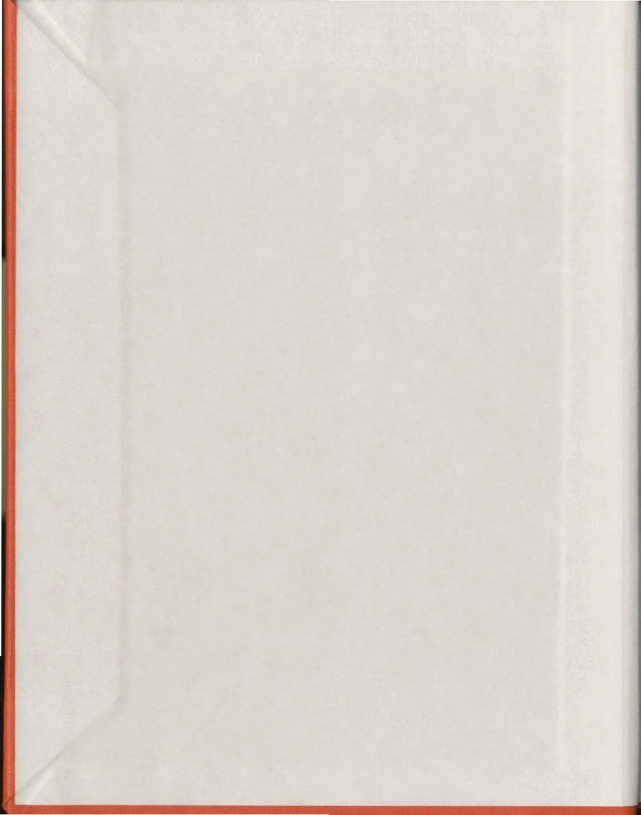
MODELLING OF ICEBERG DRIFT

CENTRE FOR NEWFOUNDLAND STUDIES

**TOTAL OF 10 PAGES ONLY
MAY BE XEROXED**

(Without Author's Permission)

MONA SALAH SHAHWAN EL-TAHAN



000233





National Library of Canada
Collections Development Branch

Canadian Theses on
Microfiche Service

Bibliothèque nationale du Canada
Direction du développement des collections

Service des thèses canadiennes
sur microfiche

NOTICE

The quality of this microfiche is heavily dependent upon the quality of the original thesis submitted for microfilming. Every effort has been made to ensure the highest quality of reproduction possible.

If pages are missing, contact the university which granted the degree.

Some pages may have indistinct print especially if the original pages were typed with a poor typewriter ribbon or if the university sent us a poor photocopy.

Previously copyrighted materials (journal articles, published tests, etc.) are not filmed.

Reproduction in full or in part of this film is governed by the Canadian Copyright Act, R.S.C. 1970, c. C-30. Please read the authorization forms which accompany this thesis.

**THIS DISSERTATION
HAS BEEN MICROFILMED
EXACTLY AS RECEIVED**

AVIS

La qualité de cette microfiche dépend grandement de la qualité de la thèse soumise au microfilmage. Nous avons tout fait pour assurer une qualité supérieure de reproduction.

S'il manque des pages, veuillez communiquer avec l'université qui a conféré le grade.

La qualité d'impression de certaines pages peut laisser à désirer, surtout si les pages originales ont été dactylographiées à l'aide d'un ruban usé ou si l'université nous a fait parvenir une photocopie de mauvaise qualité.

Les documents qui font déjà l'objet d'un droit d'auteur (articles de revue, examens publiés, etc.) ne sont pas microfilmés.

La reproduction, même partielle, de ce microfilm est soumise à la Loi canadienne sur le droit d'auteur, SRC 1970, c. C-30. Veuillez prendre connaissance des formules d'autorisation qui accompagnent cette thèse.

**LA THÈSE A ÉTÉ
MICROFILMÉE TELLE QUE
NOUS L'AVONS REÇUE**

MODELLING OF ICEBERG DRIFT

by



Moná Salah Shahwan El-Tahan

A Thesis submitted in partial fulfillment of the requirements for the
degree of

Master of Engineering

Faculty of Engineering and Applied Science
Memorial University of Newfoundland
St. John's, Newfoundland, Canada

April 1980

To My Parents

ABSTRACT

The need for a numerical model to predict iceberg drift arises primarily due to the hazards that icebergs present to the drilling vessels and platform in the offshore areas near Newfoundland and Labrador.

A dynamic model has been developed and used to study the behaviour of icebergs under different wind and current conditions.

The forces considered are due to wind, current, Coriolis effects, pressure gradients (ocean surface slope) and the acceleration of water body surrounding the iceberg. Two different techniques were used to solve the coupled non-linear differential equations of motions: 1) analog computer simulation and 2) digital computer using 4th-order Runge-Kutta method.

The validity of this model is verified by comparing the predicted and observed iceberg trajectory during a storm on August 21-22, 1972 when an oceanographic study, conducted by the Faculty of Engineering and Applied Science of Memorial University of Newfoundland, was in progress near Saglek, Labrador to monitor iceberg positions with the help of radar. The detailed wind and current data measured in-situ near the icebergs, provided a unique opportunity to verify the model and to study the effect of each of the environmental forces. Several trajectories are obtained after excluding each one of the environmental forces used in the model in order to appreciate its effect on the drift of icebergs.

In an attempt to obtain better understanding of the observed looping and spiral motions of icebergs, several trajectories are plotted

for icebergs drifting under the environmental conditions thought to be responsible for this strange behaviour. Changes in the ocean surface due to low pressure systems were found, using finite element analysis, to have no effect on the currents, and hence on the iceberg trajectory.

This study has demonstrated the importance of each of the environmental forces included in the model. A good prediction of an iceberg drift trajectory is only possible if all the environmental forces are accounted for and detailed wind and current data in the immediate vicinity of the iceberg as well as good estimates of iceberg parameters are available as input to the model.

ACKNOWLEDGEMENT

The author wishes to express her sincere thanks to Prof. D.S. Sodhi, Faculty of Engineering and Applied Science, for his guidance, encouragement and review of the manuscript.

The valuable advice and help provided by Prof. M. Booton during the sabbatical leave of Prof. Sodhi is gratefully acknowledged.

The author would like to express her appreciation to Dean R.T. Dempster for making available the iceberg data and for his encouragement.

The author is grateful to Dr. Miles McPhee of U.S. Army Cold Regions Research and Engineering Laboratory, Hanover, N.H., for his discussion which led to the successful completion of this work.

Special thanks are due to Dean Aldrich, School of Graduate Studies for providing the financial assistance.

Prof. M. El-Hawary provided valuable advice and help during analog computer programming.

The author is grateful to Mr. N. Riggs, NOROCO Ltd., St. John's, for supplying important reference material and other information.

Finally, the author would like to thank all the faculty members who acted as chairmen of the Graduate Studies Committee during her graduate studies, for their advice and encouragement, and other faculty members whose help made this study possible.

Partial support of this study from the NRC Research Grant No. A8671 is gratefully acknowledged.

TABLE OF CONTENTS

	Page
ABSTRACT	iv
ACKNOWLEDGEMENT	vi
LIST OF TABLES	ix
LIST OF FIGURES	x
 CHAPTER I. INTRODUCTION	
1.1 Background	1
1.2 Iceberg Hazards to Offshore Operations	2
1.3 Statement of the Problem	3
1.4 Thesis Outline	4
 CHAPTER II. REVIEW OF LITERATURE	
2.1 Field Studies	5
2.2 Theoretical Studies	7
2.3 Experimental Work	9
 CHAPTER III. ICEBERG DRIFT MODEL	
3.1 Mathematical Model	10
3.2 Parameters of the Iceberg Under Study	13
 CHAPTER IV. RESULTS	
4.1 Introduction	16
4.2 Drift of an Iceberg Starting From Rest in a Uniform Current	16
4.3 Study of an Iceberg Trajectory Near Saglek	18

	Page
4.4 Results	26
4.5 Discussion of Results	27
CHAPTER V. CONCLUDING REMARKS	29
TABLES AND FIGURES	30
APPENDIX A: ANALOG COMPUTER SIMULATION AND SOME PRACTICAL APPLICATIONS	
A.1 Introduction	45
A.2 Techniques of Analog Computer Simulation	45
A.3 Practical Applications	48
APPENDIX B: EFFECT OF ATMOSPHERIC PRESSURE SYSTEM ON OCEAN CURRENTS INDUCED BY CHANGES IN SEA LEVEL	
B.1 The Equation of Motion	58
B.2 Pressure Distribution	59
B.3 Practical Applications	59
B.4 Discussion and Conclusion	61
REFERENCES	70

LIST OF TABLES

Table	Page
1. Iceberg Characteristics	31
2. Wind Data (from the Log Books of C.S.S. Dawson)	32

LIST OF FIGURES

Figure	Page
1-1 Drift Pattern of Icebergs Offshore Saglek Before Pressure Disturbance	33
1-2 Drift Pattern of Icebergs After Pressure Disturbance	34
4-1 Drift of an Iceberg in Non-Dimensional Coordinates Due to Geostrophic Current For Different Values of TAD^2/F . Curves are Marked at Equal Intervals of T^1	35
4-2 Drift Pattern of Icebergs Offshore Saglek After the Storm in August, 1972 Showing Locations of Current Meters	36
4-3 Predicted and Observed Trajectories of Iceberg No. 20C During the Storm Which Passed Over the Labrador Sea on August 21-22, 1972	37
4-4 Effect of Wind Forces on Iceberg Drift	38
4-5 Iceberg Drift in Geostrophic Current With Inclusion and Exclusion of Wind	39
4-6 Effect of Iceberg Size on the Predicted Trajectory	40
4-7 Predicted Iceberg Drift With Inclusion and Exclusion of Water Acceleration	41
4-8 Effect of Coriolis Force on Iceberg Drift	42
4-9 Effect of Considering the Distribution of the Wind Generated Current Velocity Follows Ekman's Spiral on Predicted Iceberg Drift	43
4-10 Effect of Considering the Distribution of the Wind-Generated Current Velocity	44
A-1 Analog Computer Simulation of Iceberg Motion	50
A-2 Effect of Coriolis Force and Ocean Slope on Iceberg Drift Due to Geostrophic Current of 0.35 m/sec	51
A-3 Iceberg Drift Due to Rotary Current Plus a Translatory Component of 0.085 m/s Period of Rotary Current = 12 hrs	52
A-4 Iceberg Drift for Different Values of K . In a Horizontal Current $U_c = U_o \sin(\omega t)$	53
A-5 Iceberg Drift Under Coriolis Force Only for Different Initial Velocity U_o	54

Figure	Page
A-6 Effect of K on the Inertial Motion of Iceberg	55
A-7 Iceberg Drift Due to Inertial Current, Current Period = 12 hrs	56
A-8 Iceberg Drift Due to Rotary Current for Two Icebergs With Draughts Less and Greater Than the Depth of Friction Layer D_f , $UK = 0.5m/sec$	57
B-1 Finite Element Model for the Area Between the Labrador Coast and Greenland	62
B-2 Distribution of Water Velocity Along Line $U-X$ for Different Positions of Pressure Centre	63
B-3 Distribution of Water Velocity at Line $U-V$ for Different Positions of Pressure Centre	64
B-4 Water Velocity at the Centre of the Area VS. Position of Pressure Centre	65
B-5 Location of the Study Area	66
B-6 Depth Profile for the Studied Area Between Greenland and Labrador Coast	67
B-7 Water Velocity at Ocean Current Area Near Saglik VS. Position of Pressure Centre	68
B-8 Water Velocity at the Middle of the Ocean VS. Position of Pressure Centre	69

CHAPTER I

INTRODUCTION

Iceberg motion has been of interest to various groups for many years. This has been due primarily to the need for monitoring iceberg movements near shipping routes, offshore drilling platforms and buried pipelines or cables. Icebergs weighing up to ten million tons may present a threat to the development of oil exploration by disrupting or destroying offshore structures or scouring bottom buried pipelines or cables.

In spite of the serious problems they cause to the offshore petroleum industry, icebergs present a potential solution to water supply problems in a number of dry areas of the world such as the deserts of Australia, Chile and Saudi Arabia. In view of the fact that 85 per cent of the world's available freshwater resides as ice in the Antarctic and Greenland (Weeks and Campbell, 1973), the interest is presently increasing in the utilization of icebergs as a source of freshwater and other secondary applications (e.g. cold utilization).

1.1 Background

Icebergs of the Southern Hemisphere are produced by ice shelves of the Antarctic. These icebergs are mainly of tabular shapes and can be as long as 170 km. Due to their size and shape they are stable and can survive in cold water for many years.

Icebergs of the Northern Hemisphere are produced from the glaciers of Greenland, the Northeastern Canadian Arctic, Spitsbergen, the Siberian Islands and Southeastern Alaska. The areas where icebergs are most fre-

quently encountered and where they interfere most with man's activities are in Baffin Bay, the Labrador Sea and the Grand Banks of Newfoundland. These icebergs are on the average much smaller than those of the Antarctic and have very erratic shapes. Icebergs seldom exceed a few kilometers in length and by the time they reach the southern Labrador Sea they are rarely longer than one kilometer. Of about 40,000 icebergs annually produced by Greenland glaciers, only an average of 380 cross the 48°N latitude (Murray, 1969). However during the 1972 season, a record of 1,587 icebergs were counted by Ice Patrol south of 48°N latitude. Most of the icebergs drift over a period of one to two years across Baffin Bay and through the Davis Straits into the Labrador Current. This current carries the icebergs southward to the Grand Banks of Newfoundland.

1.2 Iceberg Hazards to Offshore Operations

With the exception of human error, the iceberg probably poses the largest threat to Eastern Canada's offshore oil drilling and production operations. In view of the hydrocarbon potential in the Labrador Continental Shelf and the recent discovery of oil in the Grand Banks of Newfoundland, the need has risen for year-round operations and, hence, effective protection from icebergs. Small and medium icebergs are towed away while the big ones can be avoided by moving the platform. Dynamically stationed drilling vessels can evade icebergs by fast disconnect procedures and subsea acoustic re-entries. Both strategies require a method to identify a dangerous iceberg with sufficient lead time to adopt a defensive action. Dempster (1979) suggested an operational procedure to be followed by rig operators to avoid iceberg collision using a hybrid dynamic/kinematic

prediction model.

An accurate model to predict iceberg drift will reduce the risk of collision and the time and cost of unnecessary towing of icebergs or removal of the drilling vessel.

1.3 Statement of the Problem

The purpose of this study is to develop an accurate and easy-to-handle model that can be used on the deck of a drilling vessel to predict the drift of icebergs.

A mathematical model to predict the iceberg drift trajectory has a few parameters which depend on the characteristics of icebergs (e.g. mass, area under and above water, drag coefficients in water and air), and the predicted iceberg trajectory of such a model depends largely upon the input to the model which are the environmental forces (e.g. wind and current velocities). The validity of such a model is based on the comparison of the predicted trajectory with the observed trajectory of an iceberg under any conceivable combination of forces. For this purpose, attention will be paid to the iceberg trajectories which were recorded near Saglek, Labrador, by the Faculty of Engineering, Memorial University of Newfoundland, in August of 1972 during which time a low pressure system passed over the area causing deviations from the regular iceberg tracks (Figs. 1-1 and 1-2).

Though detailed data on iceberg drift trajectories and wind velocity is available, there is limited information about the parameters of the icebergs and the current velocity near the icebergs under investigations. Under these circumstances, detailed analysis

4

is carried out on iceberg trajectories where detailed information about current data is available and an effort is made to estimate iceberg parameters using information published in the literature .

Finally the results are compared to the observed trajectories to check the validity of the model.

1.4 Thesis Outline

Chapter 1 is an introduction.

Chapter 2 presents the review of previous field, theoretical and experimental studies on iceberg drift.

Chapter 3 describes the mathematical model and the selection of the input parameters to the model.

In chapter 4 a detailed study is presented on an observed iceberg drift trajectory (#20C, Fig. 1-2) with an irregular U-turn that took place during a storm. A parametric study on an iceberg drifting in a steady geostrophic current is presented in non-dimensional coordinates.

Chapter 5 presents analysis of the observed trajectories, discussion of the results and concluding remarks.

Analog computer simulation techniques as well as some practical applications including looping and spiral motion of icebergs are presented in Appendix A.

A finite element study on the effect of changes in ocean surface elevation which are caused by low atmospheric pressure systems on the ocean current is presented in Appendix B.

CHAPTER II

REVIEW OF LITERATURE

2.1 Field Studies

Smith (1931) presented general drift patterns of iceberg motion under the influence of ocean currents and wind generated currents based on iceberg observation near the Grand Banks. Post (1956) has shown that the drift of icebergs in the North Atlantic is mainly due to the relative strengths of the Labrador current and the Gulf stream. Kollmeyer (1969), Bruneau and Dempster (1971), and Dempster and Bruneau (1973), indicated that water currents are the primary driving force. Icebergs with large draughts are found to be influenced strongly by deep steady currents while small bergs are more sensitive to wind-induced surface currents. The direct wind force on the above water portion of the iceberg is considered to be significant if the wind speed is greater than fifteen knots (7.72 m/sec) and its direction is constant for periods of the order of days.

Dempster (1974), carried out field observations on eighty icebergs and ocean currents near Saglek, Labrador, in 1972. The study indicates that the main influence on iceberg motions is the strong Labrador current, the semi-diurnal current, a secondary current resulting from a bottom effect, and, for a brief period, inertial currents resulting from the effects of a severe storm.

Russell (1973) presented field measurements of the current off the coast of Newfoundland which were found to be rotary with periods of 15.5 hrs., almost equal to the theoretical period of inertial currents. The study of measured iceberg tracks indicated that the loops made by icebergs

could be caused by inertial current effects.

Soulis (1976) studied the cross-correlation of the iceberg drift with the wind and current forces using a kinematic model to approximate the dynamic equations of motion by assuming that the iceberg velocity would be the sum of the mean current velocity and some transformation of the transitory component of the current. The study indicated that the iceberg moved 2.5 times faster than the current at depth of 13 meters.

Russell, Riggs and Robe (1977) reported on a field study on two icebergs, and on a laboratory model. In the field study two icebergs were tracked for a number of days while drogues were used to measure the currents in the vicinity. The relative drifts between the icebergs and two drogues (one near the surface and the other at a depth of 100 m) were recorded. The analysis of the results indicated that the iceberg moved more closely to the deep drogue and that no simple correlation with the local wind field was found.

Ettle (1974), reported on a field observation by the U.S. Coast Guard on eight icebergs in the period of 1965-1968. It was found that at low wind speeds the effects of permanent currents, older wind-driven currents, and tidal currents predominate over wind drag and new wind-driven currents, whereas at wind speed of over ten knots the wind has a significant effect on the drift of an iceberg. The ratio of the drag coefficient for the iceberg's above water portion to the drag coefficient for its submerged portion was found to range from 1.5 for strong winds to approximately 7 for weak winds.

Riggs, Babu, Sullivan and Russell (1979) reported on a field study

7

carried out in the summer of 1978 where four hundred icebergs were tracked by a radar station for periods of up to 275 hours. Iceberg size and shape as well as current measurement were obtained. A general relationship between the current pattern and the iceberg tracks was observed. Some iceberg tracks, however, exhibited significant looping and curving during and after the passage of low pressure systems through the area. The gyrations and periods of these loops were much larger than those reported by Dempster (1974) and Russell (1973).

Robe, Maier and Russell (1979) presented a study on five icebergs tracked by the NIMBUS-6 satellite for periods from 138 to 202 days. The icebergs observed along the Baffin Island Coast were aground from 8% to 73% of the time. Maximum daily average speeds were found to be about 0.6 m/sec. The drifts were found to be generally coastwise in a southerly direction.

2.2 Theoretical Studies

Schell (1962) estimated the drifts of icebergs due to ocean currents and wind-generated currents and indicated that wind has a significant effect on the drift of the iceberg if it continues in one direction over a long period.

Murray (1969), discussed the factors that affect the drifts of icebergs and pointed out the efficiency of the statistical approach in the determination of their drifts.

Cochkanoff, Graham and Warner (1971) studied iceberg motion under the effect of water currents and Coriolis force. An analog computer model was used to solve the differential equations of motion. In the mathematical

model, the damping force was assumed to be proportional to the square of relative velocity of water current with respect to the iceberg. The results indicated that for large Coriolis forces relative to drag and inertia forces, the motion becomes more oscillatory before approaching the current direction.

Sodhi and Dempster (1975) presented the response of icebergs due to changes in velocity of water. The equations of motion were derived by assuming that the water drag force is proportional to square of relative velocity of the water with respect to the icebergs and assuming that icebergs respond mainly to currents, thus neglecting the effect of Coriolis forces. Exact solutions were obtained for two cases - rotary tidal currents and sudden change of translatory current velocity.

Cheema and Ahuja (1978) used a kinematic model to analyze the available data on iceberg drift in the Grand Banks. In this model the velocity of iceberg is assumed to be directly proportional to current velocity. Based on the study, suggestions have been made to improve the future data collection activities.

Mountaif (1979), has developed a numerical model to predict iceberg drift. A fourth order Runge-Kutta technique was used to integrate the equations of motion which consider iceberg acceleration, the water drag, the air drag, the Coriolis acceleration and a sea surface slope term. Testing of the model over long periods of time using observed drifts of icebergs suggests that model error is somewhat random in nature and probably originated from inaccuracies in the current and wind information supplied to the model.

Napoleoni (1979) presented several numerical dynamic models for prediction of iceberg drift. In addition to the environmental loading, iceberg rotation and acceleration of water are taken into consideration for the drift trajectory prediction. The results indicated that iceberg rotation can dramatically alter the drift and that Coriolis force has significant effects on iceberg drift.

2.3 Experimental Work

Russell, Riggs and Robe (1977) described a laboratory model designed to study motions of spherical and cubical semi-immersed objects made of paraffin wax whose specific gravity was roughly the same as that of icebergs. Experiments were performed with roughened models with a trip wire attached to ensure turbulent flow in the boundary layer. The results of this study and the field study described above indicated that the values of steady-state drag coefficient, C_D , determined in the model study were lower than values normally quoted for iceberg motion. This is due to the inclusion of the inertial term in the drag force equation. It was pointed out that the practice of ignoring the inertial drag term and incorporating the inertial coefficient into the steady-state coefficient may lead to erroneous drag force calculations.

CHAPTER III

ICEBERG DRIFT MODEL

3.1 Mathematical Model

Iceberg motion is the net result of a wide spectrum of forces which vary with time and space. Some of these forces are due to gravity, pressure gradient, wind drag, water drag, Coriolis effects, waves and swells. Since this study is mainly concerned with the horizontal movement of icebergs, only the horizontal components of these forces need to be considered. Wave and swell forces are generally neglected as their magnitude is small in comparison to other forces in the horizontal directions. The mathematical model, described in the present study, takes into account the significant environmental forces due to water drag, wind drag, Coriolis acceleration and sea surface slope (pressure gradient).

The drag force due to the water drag is proportional to the square of the relative velocity of water with respect to the iceberg. The constant of proportionality depends upon the size and shape of the under-water portion of the iceberg. The current is made of many components, a few of which are the geostrophic current, the wind-driven current, inertia current and tidal current. The distribution of the magnitude and direction of the various current components varies with depth. Hence, the ocean is considered in several layers, and the water drag force is then obtained as the vectorial sum of the drag forces in terms of relative velocity of current with respect to the iceberg in each layer.

The magnitude and direction of the wind drag force depend on the size and shape of the above water portion of the iceberg. The average ratio of

the iceberg velocity to wind speed is about 0.03 (Murray, 1969), so that the relative velocity of wind with respect to iceberg is taken to be the wind velocity itself in the expression for wind drag force.

The Coriolis force, caused due to the rotating frame of reference with the Earth, tends to move the iceberg and the water surrounding the iceberg to the right of their path (clockwise) in the Northern Hemisphere. In a geostrophic current, the pressure gradient force due to a sloping sea surface balances the Coriolis force due to its movement. If the iceberg motion is not along a geostrophic current direction, there are two forces acting on the iceberg: the Coriolis force due to its movement and the pressure gradient due to the sea surface slope. In the present study, the pressure gradient force in each layer will be expressed as the negative of the current's Coriolis force (Mountain, 1979) which is equivalent to expressing the Coriolis force on the iceberg in terms of the relative velocity of the iceberg with respect to the current in a particular layer.

If the water around the iceberg is accelerating due to some forces, the same forces would also be acting on the iceberg to accelerate the iceberg. So the force balance term must include a term which takes into account the force accelerating the water mass and the iceberg at the same time, and this force on the iceberg will be equal to the product of mass of iceberg and acceleration of water surrounding the iceberg (Bayly, 1971 and Napoleoni, 1979).

The equation of motion taking all the above mentioned forces into account is written below in the component form:

$$\frac{du}{dt} = \frac{1}{M} \left[\sum_{j=1}^n \left(\frac{1}{2} C_{Dw} \rho_w A_j (U_j - u) S_j + M_j \alpha_j \right. \right. \\ \left. \left. + M_j f (v - V_j) \right) + \frac{1}{2} C_{Da} \rho_a A_a W^2 \cos \theta \right] \quad (3.1)$$

$$\frac{dv}{dt} = \frac{1}{M} \left[\sum_{j=1}^n \left(\frac{1}{2} C_{Dw} \rho_w A_j (V_j - v) S_j + M_j \beta_j \right. \right. \\ \left. \left. - M_j f (u - U_j) \right) + \frac{1}{2} C_{Da} \rho_a A_a W^2 \sin \theta \right] \quad (3.2)$$

$$\frac{dx}{dt} = u \quad (3.3)$$

$$\frac{dy}{dt} = v \quad (3.4)$$

where

- x, y = position of the iceberg (x and y axes are in the direction of east and north, respectively).
- u, v = components of the iceberg velocity in the x and y directions, respectively.
- U_j, V_j = components of the current velocity in the j th layer.
- t = time.
- M = mass of the iceberg and the added mass.
- M_j = mass of water displaced by the iceberg in the j th layer.
- C_{Dw}, C_{Da} = drag coefficient of the iceberg in water and air, respectively.
- ρ_w, ρ_a = density of water and air, respectively.
- A_j = cross-section area perpendicular to the current direc-

tion in the j th layer.

- A_a = cross-section area perpendicular to the wind direction of the above water portion of the iceberg.
- S_j = $\sqrt{(u_j - u)^2 + (v_j - v)^2}$, the relative speed of current with respect to iceberg in the j th layer.
- α_j, β_j = components of water acceleration in the j th layer.
- f = $2\Omega \sin\phi$, Coriolis parameter.
- Ω = angular velocity of Earth rotation.
- ϕ = latitude.
- w = wind speed.
- θ = direction of wind measured anti-clockwise from x axis.

If the parameters related to the iceberg are known, the above set of equations may be integrated provided the current and wind data are supplied as the forcing function (or input to the model) to obtain the response of the model in the form of the iceberg velocity and position. Since the set of differential equations are coupled and non-linear, it is expeditious to integrate them with the help of a digital computer or an analog computer, and both of these computers are used in the present study. The details of the analog simulation are given in Appendix A. The 4th order Runge-Kutta method is used to integrate the set of equation, 3.1-3.4, with the help of a digital computer (PDP 11/40) along with a plotting facility.

3.2 Parameters of the Icebergs Under Study

Since the mass, area and drag coefficients of the icebergs under study are not known, these values are chosen from the range of values quoted in literature, and this section describes the manner in which the parameters used in the present study are selected.

a) Drag Coefficients

It has been shown by Hoerner (1965) that the drag coefficients in water, C_{Dw} , and in air, C_{Da} , depend on the Reynolds number, R_e . The values of R_e for icebergs are of the order of 10^7 (International Ice Patrol, 1960). The studies reported by the International Ice Patrol indicated that the drag coefficients must be higher than 0.2 but not higher than 1.0 and that the drag coefficient ratio for in air to water lies between 1.0 to 1.5. Eittle (1974) found that this ratio ranges from 1.5 for strong winds to about 7 for weak winds. In a study on iceberg towing Chirivella and Miller (1978) found out that R_e for in water is about 9×10^8 and for in air ranges from 10^7 to 10^9 and the corresponding values of C_{Dw} and C_{Da} are 1.0 and 0.9 respectively. Banks and Smith (1974) towed small icebergs on the Labrador Coast and obtained 1.2 as a mean value for C_{Dw} with a standard deviation of 0.2. Similar studies carried out by Weeks and Campbell (1973) on large icebergs indicated values of 0.6 to 0.9. In another iceberg towing experiment, Dempster (1979) found that a value of C_{Dw} taken as 0.5 to 0.7 produce the correct trends of motion but a value of 2.0 achieved the best fit between the computed and actual data. The high value of C_{Dw} , in his opinion is probably a composite of a drag coefficient and a correction factor to compensate for errors in the estimation of the system parameters.

Russell et al (1977) indicated that values of C_{Dw} that must be used in prediction of iceberg drift are usually very high because steady-state conditions are assumed. Such steady-state conditions are impossible to take place unless there is no relative motion between the iceberg and the water in which case the drag force is zero. Instead, the iceberg must accelerate and decelerate continuously. They concluded that the practice of ignoring

the inertial drag term and incorporating the inertial coefficient into the steady-state coefficient may lead to erroneous drag force calculations.

It can be concluded that water drag coefficient for iceberg calculations ranges between 0.6 to 1.2 and that the ratio C_{Da} / C_{Dw} is somewhere around 1.5.

It has been decided to use a value of C_{Dw} of 1.0 and C_{Da} of 1.5 regardless of the size and shape of the iceberg.

b) Added Water Mass

The concept of "added water mass" is introduced to account for inertial drag. Inertial drag arises because of the acceleration of the fluid around the object. The object behaves as if a mass were added to it. The added water mass can be determined from the potential flow theory.

The added mass in our model is assumed to be half the mass of iceberg which agrees with measurements made by Hamilton and Lindell (1971) and calculations made by Lamb (1879) for spherical and cubic objects.

c) Iceberg Mass and Cross-Sectional Area

Iceberg parameters needed for the model are the mass and the cross-sectional area in each water layer and in the air (Eqn. 3.1). This information cannot be obtained operationally for each iceberg. Instead observations made over a number of years have been used to establish seven classes of icebergs which could be distinguished from aircraft. Table 1 presents the average areal and mass characteristics for each class as published by Mountain (1979). Iceberg parameters needed for this study are chosen from this table.

CHAPTER IV

RESULTS

4.1 Introduction

In the first part of this chapter, a parametric study of the iceberg drift model is presented in which the trajectory is obtained for an iceberg drift in a steady current starting from rest. This study shows the dependence of the iceberg trajectory on the parameters obtained by writing the equations of motion in a non-dimensional form.

In the second part of this chapter, the verification of the iceberg drift model, presented in the previous chapter, is attempted by comparing the trajectories predicted by the model with that of iceberg #20C observed near Saglek, Labrador, in 1972. The data used as input to the model are the current and wind data obtained in the field. The comparison between the predicted and observed iceberg trajectories is good.

4.2 Drift of an Iceberg Starting from Rest in a Uniform Current

Iceberg grounding is a frequent occurrence, and in fact icebergs have been observed to remain grounded for the 40% of the observation time (Robe, Maier and Russell, 1979). The icebergs sometimes become loose and start drifting again which provides the motivation of this study. The trajectory of an iceberg under the influence of only a uniform and steady geostrophic current in the x-direction, U, is governed by the following equations of motion which are obtained from equations 3.1 and 3.4 assuming the water column to have a constant velocity at all depths.

$$\frac{du}{dt} = \kappa(U-u) \sqrt{(U-u)^2 + v^2} + fv \quad (4.1)$$

$$\frac{dv}{dt} = -\kappa v \sqrt{(u-u')^2 + v'^2} - f(u-u') \quad (4.2)$$

$$\frac{dx}{dt} = u \quad (4.3)$$

$$\frac{dy}{dt} = v \quad (4.4)$$

where

$$\kappa = \frac{C_{Dw} \rho_w A}{2M}$$

the initial values of x , y , u and v are assumed to be zero at the beginning of the integration process. The above set of equations can be written in a non-dimensional form as given below:

$$\frac{du'}{dt'} = (1-u') \sqrt{(1-u')^2 + v'^2} + \tau f v' \quad (4.5)$$

$$\frac{dv'}{dt'} = -v' \sqrt{(1-u')^2 + v'^2} + \tau f (1-u') \quad (4.6)$$

$$\frac{dx'}{dt'} = u' \quad (4.7)$$

$$\frac{dy'}{dt'} = v' \quad (4.8)$$

where $t = 1/U\kappa$, $u' = u/U$, $v' = v/U$, $t' = t/\tau$, $x' = x\kappa$ and $y' = y\kappa$.

The positions of the iceberg (x' , y') are plotted for various values of τf in Fig. 4-1. The positions of the icebergs are marked after intervals of $t' = 2$. The parameter τf takes into consideration the Coriolis factor and the iceberg characteristics such as mass, area under water, density and drag coefficient. The range of values assumed for τf have been computed from the values given in Table T for area and mass of icebergs.

These plots are similar to those obtained by Cochkanoff, et al (1971) using analog simulation of the problem. The initial motion is the resultant of the forces due to the water drag, and the pressure gradient (the sea

surface slope) caused by the geostrophic current. As the iceberg picks up speed, the drag force decreases, and the Coriolis force increases to counterbalance the pressure gradient force. The initial wavy motion of an iceberg as depicted by curve 5 in Fig. 4-1 is the result of interaction of the pressure gradient force and the Coriolis force. After a long time from the start of the iceberg motion, the trajectories become straight in a steady-state drift.

4.3 Study of an Iceberg Trajectory Near Saglek

In August of 1972, the Faculty of Engineering and Applied Science of Memorial University of Newfoundland conducted an oceanographic investigation collecting data on iceberg drift, currents and winds. A full account of their activities has been described by Allen (1972). Icebergs were tracked using a radar installed in a shore station at Saglek, Labrador, while the C.S.S. "Dawson" provided by the Bedford Institute of Oceanography, together with the Canadian Armed Services, Maritime Command, collected oceanographical and meteorological data in the vicinity. A total of one hundred and ten icebergs were tracked, some for several days and others for only several hours. The scientific party aboard the "Dawson" obtained extensive data on currents at four locations as shown in Fig. 4-2. The current meters were installed at depths of 13m and 75m at each of these four locations, and three additional current meters were installed 10m above the sea bottom at locations A, B and C, shown in Fig. 4-2. The data obtained from the current meters is presented and analyzed by Holden (1974). His conclusions are that the current at Saglek oscillated with the tidal period of 12.5 hours before the storm of August 22, 1972, and the oscillation period after the storm was inertial for current meters

close to the surface of water. This suggests that the storm influenced the flow conditions in the oceanic boundary layer.

The iceberg drift trajectories obtained before, during and after the storm along with the current and wind data present a unique opportunity to test the iceberg drift model. The information related to the shape, mass and areas above and below water of the icebergs under investigation are not available, and reasonable values of these parameters have been assumed from the data quoted in the literature (Mountain, 1979).

In the following, we present the results of two studies based on this set of data and their main conclusions. Later, the discussion is continued with the results of the present study.

a) Soulis (1976) used the drift data of approximately 33 icebergs to determine a vector cross-correlation between the iceberg drift velocity and the wind and current data. Although detailed behaviour of an iceberg is highly individual, Soulis (1976) concluded that, in general, "the iceberg studied:

- 1) moved 2.5 times faster, but in the same direction as, the mean current experienced by the iceberg at a depth of 13 meters.
- 2) had a transitory velocity component which equalled 0.5 of the transitory current experienced by the iceberg at a depth of 13 meters and lagged 73° .
- 3) had a wind-induced velocity component equal to 4% of and 25 degrees to the right of, the wind velocity."

The above conclusions by Soulis (1976) have been arrived at by correlating the iceberg drift velocity with the current data obtained at 13

meters depth. These results should be used with care because an iceberg extends below the oceanic boundary layer which is about 30 to 40 m deep, and the current data on the 13 meter level would be an indicator of current composition in the boundary layer only. A similar cross-correlation between the iceberg velocity vectors and the wind and deeper current velocity was not attempted perhaps due to malfunctions of the two current meters at 75 meters below sea surface level. However, all the current meters 10 meter above sea bottom were operational and, perhaps, cross-correlations between the current data obtained from those current meters and the iceberg drift velocity may have been meaningful.

b) Dempster and Bruneau (1973) have given a general explanation that the icebergs move under the influence of currents which cause them to have trajectories in the form of loops and spirals when there is weak or no wind. As mentioned earlier, the storm which moved over the area on August 21-22, 1972, caused considerable disturbance in the trajectories of four icebergs. Dempster and Bruneau (1973) suggested an explanation for these deviations to be the effect of currents set up due to changes in the sea surface elevation as the low atmospheric pressure zone passed over the area. For a motionless sea and homogeneous water, the change in height (h) of the sea surface is related to the change in the atmospheric pressure (P_a) by the expression (Neumann and Pierson, 1966).

$$\Delta h(\text{cms}) = -\Delta P_a \quad (\text{mbars}) \quad (4.9)$$

The above expression shows that in the areas of low atmospheric pressure the sea surface level must be higher than the mean sea level, and vice versa. Although the inverse pressure law is not strictly applicable to a dynamic, non-homogeneous ocean, it does give an indication of magnitude.

of disturbance caused by an atmospheric pressure.

When the sea surface level changes, the currents are set up to satisfy continuity, and the equation of continuity is written below (Neumann and Pierson, 1966):

$$\frac{\partial u}{\partial x} + \frac{\partial v}{\partial y} = \frac{1}{h} \frac{\partial \eta}{\partial t} \quad (4.10)$$

where u and v are the horizontal water velocities in the x and y directions, h the depth of ocean and $\eta(t)$ is the change of sea surface level above the mean level at a particular time t . During the storm, the atmospheric pressure fell by a total of 36 to 38 millibars in about 6 to 8 hours which would result in a very low rate of change in sea surface elevation $\left(\frac{\partial \eta}{\partial t}\right)$. Further, the depth of ocean is in the order of 100m and more which makes the right hand side of equation 4.10 insignificant. A detailed finite element analysis was undertaken to solve equation 4.10 taking various ocean depths into consideration, and the results show that the currents developed due to changes in sea surface level are negligible when the ocean depth is in the order of 100 meters for the same approximate conditions as those prevailed during the storm. The details of this study are given in Appendix B.

c) Present Study

The only other reason for the complex iceberg trajectories during the storm can be the direct action of the wind on the sails of the icebergs and the indirect action of wind on the oceanic boundary layer resulting in wind driven currents which in turn affect the iceberg motion. Figure 4-3 shows the contours of atmospheric pressure system before and after the crossing of the storm centre through Sagiek, and it also shows

the reversal of wind directions during the storm. It is for this purpose the present study is undertaken to develop an iceberg drift model and compare the predicted iceberg trajectories to the observed ones. The sources of these data used to run the model are given below.

(1) Currents

As mentioned earlier, the current data is obtained from meters installed at four locations, A, B, C and D (shown in Fig. 4-2) and at three different levels below the sea surface level (A_1, B_1, C_1 and D_1 at 13m, A_2, B_2, C_2 and D_2 at 75m and A_3, B_3, C_3 10 meter above sea floor, which are 165m, 146m and 176m below the sea surface at locations A, B and C, respectively). The current meters A_2 and B_2 recorded only the current direction and not the magnitude due to some malfunction of this instrument. The data used for running the iceberg drift model uses the directions measured by A_2 and B_2 and the magnitudes measured by A_3 and B_3 . This is justified because the magnitude of the geostrophic current is approximately constant between the top and the bottom oceanic boundary layers.

Since the iceberg drift model considers the water column in two layers, the ocean boundary layer extending from the ocean surface to about 40 meters depth and the deeper layer from 40 meter depth to the ocean bottom, the current in the deeper layer is assumed to be geostrophic and constant with respect to depth for our calculations whereas the current in the boundary layer is assumed to be the vectorial sum of geostrophic and wind driven currents. Assuming that the structure of the wind driven currents to be in the form of an Ekman spiral, we can derive the information about the direction and magnitude of the water mass transport from the current meter data located in the boundary layer and in

deeper water.

If the wind shear stress vector is acting in the +y direction (i.e. to the north), the wind driven current velocity components to the east and north, u and v, are given by the following expression (Neumann, 1968).

$$\begin{aligned} u &= V_0 e^{-(\pi/D)Z} \cos(45^\circ - \pi Z/D) \\ v &= V_0 e^{-(\pi/D)Z} \sin(45^\circ - \pi Z/D) \end{aligned} \quad (4.11)$$

where $D = 36.7m/\sqrt{\sin\phi}$, V_0 represents the speed of the surface current, Z the depth below the water surface and ϕ the latitude of the location. The above current distribution is known as the "Ekman Spiral".

The latitude of Sagley is $58.5^\circ N$, and the depth of boundary layer $D=39.7$ meters which is approximately equal to the depth of mixing layer as is evident from the contour lines of the measured STD data (Allen, 1972). The net water mass transport, S_x and S_y in the easterly and northerly directions across 1 cm. width are given by (Neumann, 1968).

$$\begin{aligned} S_x &= \rho \frac{V_0 D}{\pi\sqrt{2}} \\ S_y &= 0 \end{aligned} \quad (4.12)$$

This is a remarkable result which states that total water mass transport is directed 90° to the right of the wind shear stress direction in the Northern Hemisphere and to the left of the wind shear stress vector direction in the Southern Hemisphere. The net effect of wind driven currents on the motion of an iceberg is to integrate the drag forces at different levels in the boundary layer. In this thesis, it is assumed that the boundary layer has a uniform velocity such that the net water mass trans-

port is equal to that given in equation 4.12 and the direction is 90° to the right of the wind shear stress vector. Thus, the average water velocity component in the boundary layer is $\bar{u} = 0.225V_0$ and $\bar{v} = 0$. Using equations 4.11, the velocity components at 13m below the sea surface level are:

$$u = 0.358 V_0 \cos(-13.9^\circ)$$

and

$$v = 0.358 V_0 \sin(-13.9^\circ)$$

Hence, we obtain a factor, equal to 0.628, which is the ratio of the magnitudes of the average velocity in the boundary layer to that at 13m level, and the difference between their directions is 13.9° .

The following procedure is followed to calculate the input data for the currents in the model described in Chapter 3 to predict the iceberg drift trajectories. Let the measured velocity components at the 75 meter depth be designated as U_g and V_g in the easterly and northerly directions, respectively, and let U_s and V_s be the designation given to the velocity data at 13 meter depth. The iceberg drift model needs the input current velocities at two layers of the water column U_1, V_1 in the boundary layer and U_2, V_2 in the deeper layer. For the deeper layer, the input velocity data is taken to be the same as the measured velocity, i.e. $U_2 = U_g$ and $V_2 = V_g$. The average water velocity components for the boundary layer are taken as follows:

$$\begin{aligned} U_1 &= 0.628[(U_s - U_g) \cos(13.9^\circ) - (V_s - V_g) \sin(13.9^\circ)] + U_g \\ V_1 &= 0.628[(U_s - U_g) \sin(13.9^\circ) + (V_s - V_g) \cos(13.9^\circ)] + V_g \end{aligned} \quad (4.13)$$

The equation 4.13 effectively performs the operations of adjustment of magnitude and direction on the vector of the wind generated current velocity and then adding the geostrophic components to obtain the average velocity in the boundary layer.

Since the current velocity vary spatially as well as temporally, the current data is interpolated from the currents values at corresponding depths at locations A and B to predict the trajectory of a particular iceberg designated as 20C whose drift path happened to be close to the current meters. A cubic interpolation function is used to give more weight to the current meter closer to the iceberg:

$$U_{\text{interpolated}} = U_A F + U_B (1-F)$$

$$\text{where } F = 3\xi^2 - 3\xi^3, \quad \xi = (Y_1 - Y_B)/(Y_A - Y_B)$$

U_A, U_B = data from current meters at A and B, respectively.

Y_1, Y_A, Y_B = ordinates of the iceberg position and locations A and B, respectively.

(ii) Wind Data

At first, the wind data was obtained from the atmospheric pressure charts obtained from Environment Canada (Gender office). The interpretation of these six hourly atmospheric pressure data was done by an experienced meteorologist (Mr. Duncan Finnyson of NORDCO Ltd., St. John's). The wind data thus obtained gave a good idea of the wind speed and directions.

As more detailed wind speed and direction at the sea surface are required to run the iceberg drift model, we obtained the wind data from the log books of C.S.S. "Dawson" where such data was recorded at 2 to 4

hours interval. A linear interpolation is used to deduce the wind speed and direction at an intermediate time.

4.4 Results

Since the mass and other parameters of the iceberg are not known, the trajectories of iceberg drift are obtained using small, medium and large non-tabular icebergs as given in Table 1, and Figs. 4-4 and 4-5 show the predicted trajectories along with the observed trajectory of iceberg #20C during the storm which passed over the area on August 21-22, 1972. The predicted trajectory of a medium non-tabular iceberg (Fig. 4-4) gives a good fit to the observed trajectory, and thus the iceberg #20C is assumed to be a medium non-tabular iceberg.

Fig. 4-6 shows two predicted iceberg trajectories when the iceberg is driven by the wind alone and by the currents alone. Fig. 4-7 shows two iceberg trajectories when the iceberg is driven by geostrophic currents only and by geostrophic currents and wind together. In these two figures, the effect of excluding a particular environmental force, can be seen as the observed iceberg trajectory is also shown there. It is evident from these results that currents and wind have significant effect on the iceberg drift.

Fig. 4-8 shows the effect of including and excluding the Coriolis force on the predicted iceberg drift trajectory. The Coriolis force must be included in the calculations for a good prediction of iceberg trajectory. Fig. 4-9 depicts the effect of including and excluding the water acceleration in the drift model. Though the net effect of excluding water acceleration term is not large, a better drift trajectory is obtain-

ed in this case by including the water acceleration term in the model.

Finally, Fig. 4-10 depicts two predicted iceberg drift trajectories when equation 4.13 is used to estimate the average water velocity in the boundary layer and when the current data at 13 meter depth is used as obtained (i.e., $U_1 = U_s$ and $V_1 = V_s$). As it is evident from the results, the current data at 13 meters depth alone does not give a good prediction of iceberg drift, and this data along with data at 75 meters depth has to be used to estimate the wind generated current in the boundary layer.

4.5 Discussion of Results

As mentioned earlier, one of the objectives of this investigation is to analyze the observed drift trajectories to find some interpretations of some of the observed strange behaviour of icebergs (looping, spiral motion and irregular U turns). A detailed study is presented in the previous section on the observed iceberg drift trajectory #20C with an irregular U-turn that took place during the storm. This study was feasible because the iceberg moved in the vicinity of two current meters (Fig. 4-2) and, hence detailed data on currents could be obtained. Unfortunately, no similar data is available for iceberg trajectories with loops. The looping motion either took place in locations far away from current meters (e.g., tracks #10F, 11L and 13G in Fig. 1-1, and 17B, 17D and 19B in Fig. 4-2) or close to a current meter but at a time where no current data is available (e.g. track #7M, Fig. 1-1). Therefore, detailed analyses, similar to that performed on trajectory #20C, can not be carried out for other trajectories. However, a better understanding of the looping motion can be obtained by studying the behaviour of iceberg under the same environmental conditions suggested to cause looping motion and other conditions under which icebergs

were reported to have spiral and looping motions. A detailed account of this study is presented in Appendix A, and the behaviour of icebergs during the storm that passed over Saglek on August 21-22, 1972 is discussed below.

Fig. 4-2 presents some of the iceberg trajectories that were disturbed by the storm. Generally speaking the icebergs moved back and forth forming either U-turns (#20C and 20D), or loops (#17B, 17D and 19B). The trajectories with U-turns were close to Saglek while the others were far to the north. This difference in iceberg behaviour seems to be due to difference in local current field. However, the direct action of the wind on the sails of the icebergs is evident from the fact that icebergs moved back and forth as the wind direction changed due to the passage of the storm centre through the area (Fig. 4-3), and that the deviation from the regular drift trajectories start and stop at about the same time (Fig. 4-2).

Availability of detailed current and wind data for iceberg #20C presented a unique opportunity to verify the validity of our model and to evaluate the significance of each of the forces included in the model (air drag, water drag, water acceleration and Coriolis force). The predicted drift trajectory of an iceberg is significantly influenced by the size of iceberg (Figs. 4-4 and 4-5). The assumption that iceberg #20C is a medium non-tabular iceberg is supported by visual observations made by Dempster (Personal Communication, 1980). The results presented in Figures 4-6 to 4-9 demonstrate the importance of each of these forces.

Due to the non-uniform distribution of the current velocity in the ocean boundary layer, the current data in the boundary layer along with data at deeper depths should be used to estimate the average velocity in the boundary layer for good prediction of the iceberg drift (Fig. 4-10).

CHAPTER V

CONCLUDING REMARKS

A dynamic model to predict iceberg drift has been developed and verified by comparing the predicted iceberg trajectory to that observed during a storm. Changes in ocean surface elevation due to a low atmospheric pressure system have no effect on ocean current in deep water depths as in the case near Saglek. The direct action of wind is the main cause of the observed back and forth motion of icebergs during the storm. The indirect effect of wind on the motion of icebergs is via wind-generated current and the changes in geostrophic current, if any.

Iceberg trajectories with loops and spiral motion were obtained under simulated conditions. However, no general conclusion to the cause of this behaviour can be drawn mainly because of the absence of the in-situ wind and current measurements for trajectories with such behaviour.

To our knowledge, this is the first published study where an iceberg drift model is tested during a storm using detailed current and wind data measured in the immediate vicinity of an iceberg. From this study it is evident that the physics of the iceberg drift model is known to extent that a good prediction of an iceberg trajectory during a storm can be made provided detailed current and wind data are available as input to the model.

It is recommended that a model to predict ocean currents is needed to generate the necessary data on currents which is to be input into the iceberg drift model. In the absence of such a model, the current data must be obtained by a string of current meters in the vicinity of a location where icebergs may be a threat to a particular installation.

TABLES AND FIGURES

Table 1. Iceberg Characteristics (Mountain, 1979)

Iceberg Type	Size	Mass (10^6 kg)	Dry Area (M^2)	Net Area (M^2) Per Depth Layer			
				0-20M	20-50M	50-100M	100-120M
NON TABULAR	Growler	.45	10	80	0	0	0
	Small	.75	230	780	870	0	0
	Medium	900	910	1800	1900	2700	0
	Large	5500	2000	3500	3750	5300	1400
TABULAR	Small	245	650	1900	2600	0	0
	Medium	2170	2700	4400	5900	8700	0
	Large	8235	5200	7200	9700	14,400	5,000

Table 2. Wind Data
 (From the Log Books of C.S.S. Dawson)

Date	GMT	Wind Speed (kts)	Wind Direction
August 20	0500	8	200
	0700	5	210
	1100	10	200
	1500	15	230
	1900	17	030
August 21	0300	10	240
	0500	9	150
	0700	9	150
	1100	15	120
	1500	25	135
	1800	30	125
	1900	27	125
	2100	20	320
	2300	20	320
August 22	0100	10	240
	0300	25	280
	0500	30	280
	0700	30	275
	0900	50	270
	1100	36	265
	1300	35	280
	1500	28	265
	1700	26	280
	1900	20	285
	2100	18	260
2300	18	260	

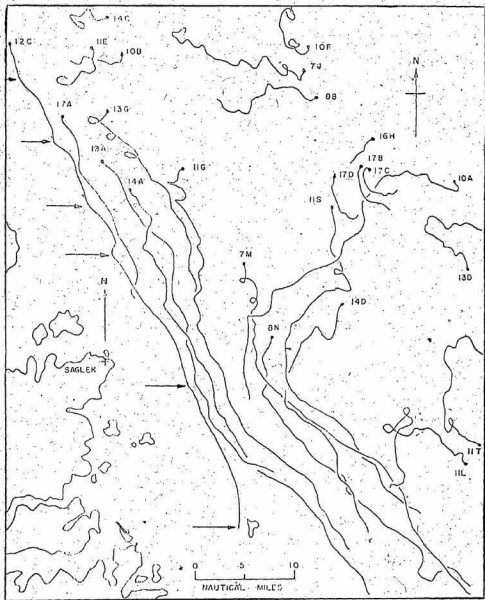


FIG. 1.1 DRIFT PATTERN OF ICEBERGS OFFSHORE SAGLIK BEFORE PRESSURE DISTURBANCE. (DEMPSTER AND BRUNEAU, 1973)

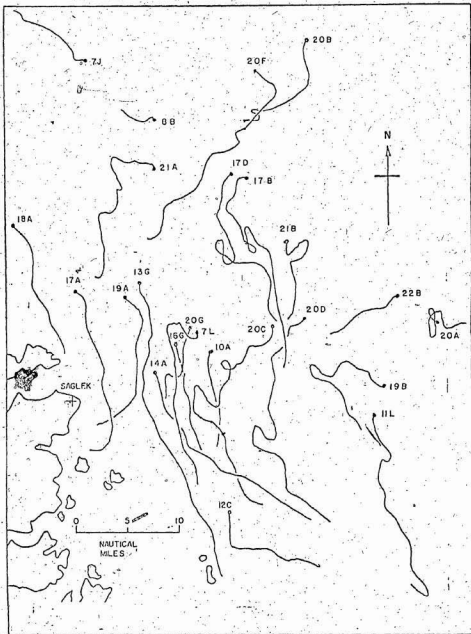


FIG. 1.2 DRIFT PATTERN OF ICEBERGS AFTER PRESSURE DISTURBANCE.
(DEMPSTER AND BRUINEAU, 1973)

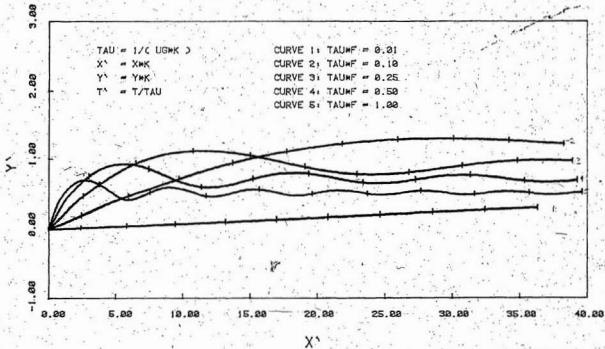


FIG. 4.1 DRIFT OF AN ICEBERG IN NON-DIMENSIONAL COORDINATES DUE TO GEOSTROPHIC CURRENT FOR DIFFERENT VALUES OF τu_{MF} . CURVES ARE MARKED AT EQUAL INTERVALS OF T' OF 2.

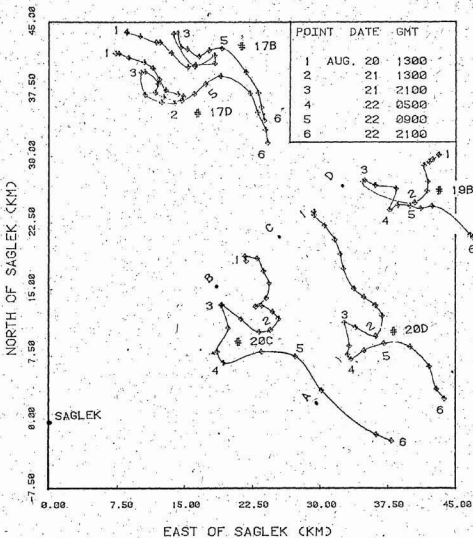
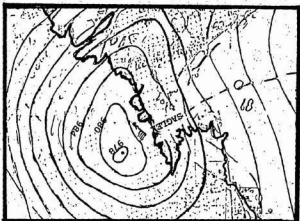


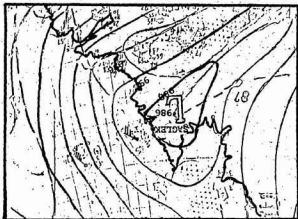
FIG. 4.2 DRIFT PATTERN OF ICEBERGS OFFSHORE SAGLEK AFTER THE STORM IN AUGUST 1972 SHOWING LOCATIONS OF CURRENT METERS.

FIG. 4.3 CONTOUR LINES OF ATMOSPHERIC PRESSURE SYSTEM AS THE CENTER OF THE STORM PASSED THROUGH SAGLEK.

AUGUST 22, 1972 - 0000 GMT.



AUGUST 21, 1972 - 1800 GMT.



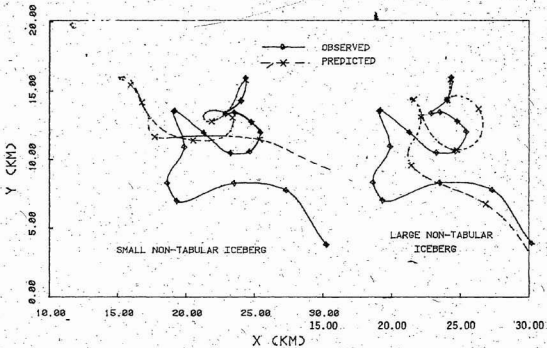


FIG. 4.5 EFFECT OF ICEBERG SIZE ON THE PREDICTED TRAJECTORY.

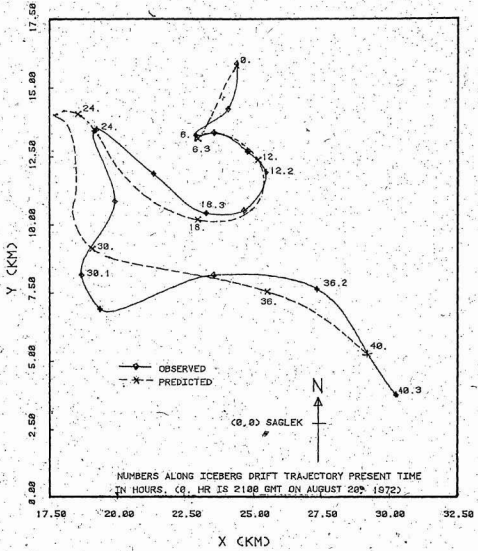


FIG. 4.4 PREDICTED AND OBSERVED TRAJECTORIES OF ICEBERG #20C DURING THE STORM WHICH PASSED OVER THE LABRADOR SEA ON AUGUST 21-22, 1972.

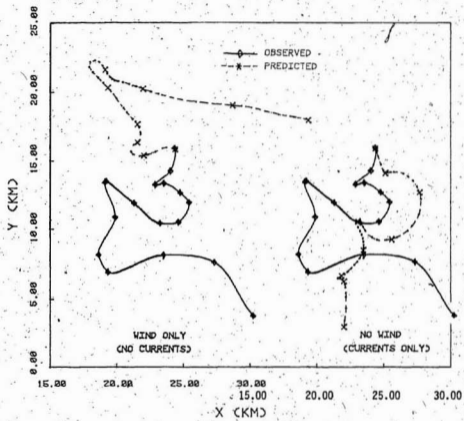


FIG. 4.6 EFFECT OF WIND FORCES ON ICEBERG DRIFT DURING STORM.

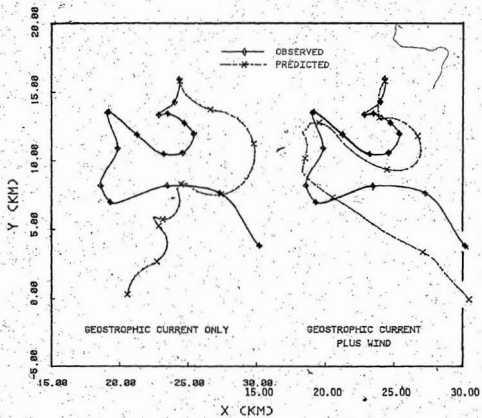


FIG. 4.7 ICEBERG DRIFT IN GEOSTROPHIC CURRENT WITH INCLUSION AND EXCLUSION OF WIND.

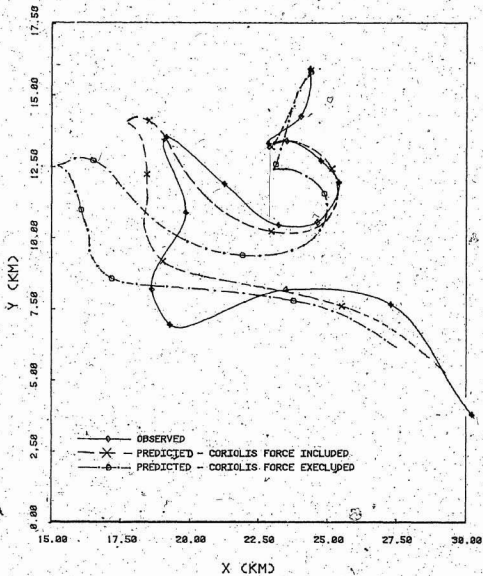


FIG. 4.8 EFFECT OF CORIOLIS FORCE ON ICEBERG DRIFT.

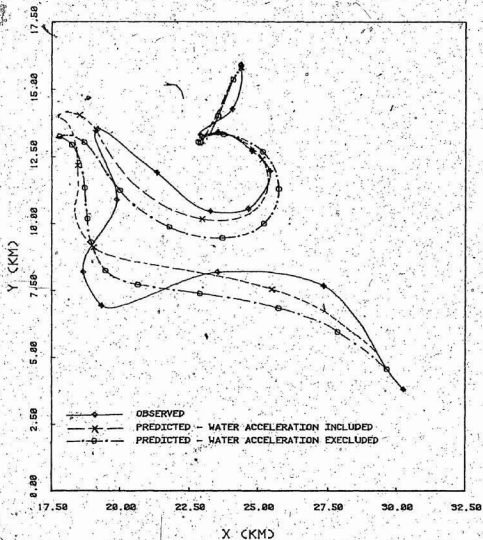


FIG. 4.9 PREDICTED ICEBERG DRIFT WITH INCLUSION AND EXCLUSION OF WATER ACCELERATION.

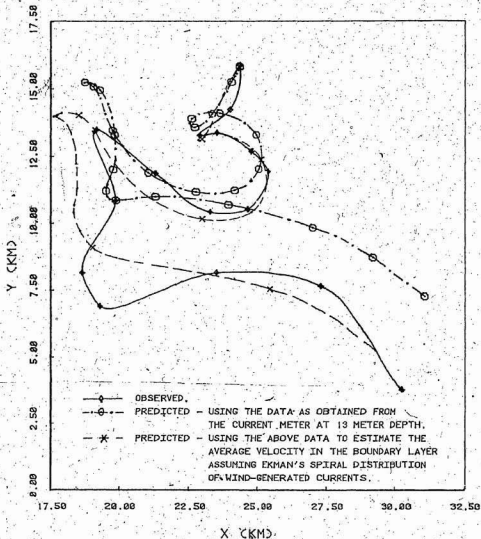


FIG. 4.10 EFFECT OF CONSIDERING THE DISTRIBUTION OF THE WIND-GENERATED CURRENT VELOCITY.

APPENDIX A

ANALOG COMPUTER SIMULATION

AND

SOME PRACTICAL APPLICATIONS

A.1 Introduction

One of the major benefits of analog processing is the ability to modify parameters during problem execution while observing its quantitative effects on a variable. In studying iceberg drift problems, this is particularly true when the program is being run in high-speed repetitive operation with the iceberg drift being graphically displayed. Typically, one can alter a coefficient value (e.g. iceberg parameter, current parameter, wind parameter, --- etc) while observing its effect on the iceberg drift. This technique presents a fast and efficient way to produce an iceberg drift trajectory similar to an observed track. This can be used to find an interpretation of the strange iceberg behaviour, e.g., looping after a storm. It can also be used to determine one of the model parameters (iceberg parameters, wind or current data) if the rest of the parameters and the iceberg track are known.

A.2 Techniques of Analog Computer Simulation

Problem solution by analog computers is accomplished by analogy, that is, the computer is programmed so that its circuit equations have the same mathematical form as the equations of the problem. In this type of computer, voltages represent various physical quantities, such as acceleration, force, displacement and so on. It is necessary, therefore, to arrange the voltages that present these variables and their

rates of change such that they will never have values larger than the voltage limitations of the computer (± 10 volts), nor such that they will ever change rapidly enough to exceed the frequency of the computer and its recording equipment. The generally accepted duration of a solution run is some where between 15 and 60 sec. (Jeness, 1965). If the solution takes too long, errors due to integrator drift will be introduced. On the other hand, if the solution time is too short, the permissible frequency limitations of the components and recording equipment may be exceeded. Keeping the maximum values of variables, their rate of change in the analog model, and the duration of the solution within the above-mentioned limitations is accomplished by "amplitude scaling" and "time scaling". The techniques of time and amplitude scaling described by Zulauf (1966), Rehoff (1967), and Hausner (1971) were used in scaling the analog variables.

To illustrate the analog simulation of the equation of motion and the scaling techniques, let us consider the case of an iceberg moving under geostrophic current. Considering the corresponding ocean surface slope and assuming no-wind condition, the equations of motion become:

$$\frac{du}{dt} = \kappa(U_g - u) \sqrt{(U_g - u)^2 + (V_g - v)^2} - f(V_g - v) \quad (\text{A.1})$$

$$\frac{dv}{dt} = \kappa(V_g - v) \sqrt{(U_g - u)^2 + (V_g - v)^2} + f(U_g - u) \quad (\text{A.2})$$

$$\text{where } \kappa = \frac{C_D \rho_w A}{2M} \quad (\text{A.3})$$

Time and amplitude scaling were chosen so that the length unit is 10 km

and time unit is one hour. This means that one second of the computer time represents a real time of one hour. A unit length in the model is equivalent to a real distance of 10 km. The length scale is 1 km/volt and velocity scale is (1 km/hr)/volt.

Having chosen these scales, then the requirements of the voltage and frequency limitations of the analog computer components are fulfilled. However, the maximum value of κ (Eqn. A.3) is approximately 24 which corresponds to a voltage of 240 (10 volt = unity). In order to keep the value less than unity (less than 10 volt), equations A.1 and A.2 can be rewritten as:

$$\frac{du}{dt} = \kappa' (5U_g - 5u) \sqrt{(5U_g - 5u)^2 + (5V_g - 5v)^2} - f' (5V_g - 5v) \quad (\text{A.4})$$

$$\frac{dv}{dt} = \kappa' (5V_g - 5v) \sqrt{(5U_g - 5u)^2 + (5V_g - 5v)^2} + f' (5U_g - 5u) \quad (\text{A.5})$$

where

$$\kappa' = \frac{\kappa}{25} \quad \text{always} < 1 \quad (\text{A.6})$$

$$f' = \frac{f}{5} \quad \text{always} < 1 \quad (\text{A.7})$$

So all the maximum values of the variables and coefficients in the analog model are kept below unity (less than 10 volt). The analog computer simulation of the above equations of motion is presented in Fig. A-1.

The programme circuit was patched on the patching panel of the computer. An oscilloscope and an x-y plotter were used to display and

plot iceberg drift and the time history of iceberg velocity.

A.3 Practical Applications

a) Effect of Coriolis and Pressure Gradient Forces

Some kinematic and dynamic models developed to predict iceberg drift ignore either Coriolis force or ocean slope (pressure gradient), or both. To estimate the error involved in such practice, iceberg drift in a geostrophic current is obtained for the different cases shown in Fig.

A-2. Coriolis force acts in $-y$ direction and the slope force in $+y$ direction. The results indicate that ignoring Coriolis force, ocean slope, or both leads to erroneous prediction of iceberg drift. The error is significant and increases as time increases.

b) Iceberg Drift in a Rotary Currents with Translatory Component

This kind of current has been observed and recorded by several investigators (Neumann, 1968). The iceberg trajectories are in the form of loops, the size of which and the distance between them are function of the ratio of the rotary to the translatory components. For large ratios, loops are large and close to each other. Fig. A-3 shows an example of iceberg drift under such conditions. Only one loop is shown in each case. Similar, but larger, loops in the iceberg drift have been observed by Riggs, et al (1979) in Lancaster Sound, Baffin Bay in summer of 1978.

c) Iceberg Drift in a Periodic Current

Fig. A-4 shows iceberg drift due to a horizontal current with velocity time history given by:

$$U_c = U_o \sin \omega t \quad (A.8)$$

The tidal movement of water in the Strait of Belle Isle has this type of velocity function. The iceberg moves in an elliptic loop the width of which is a function of the coefficient κ . Loop size is larger for large icebergs.

d) Inertial Motion of Iceberg

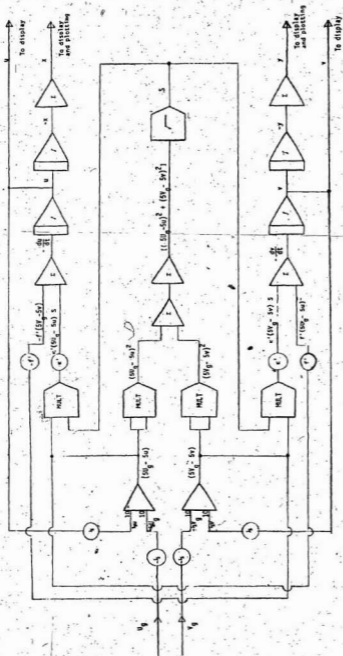
Fig. A-5 shows iceberg's motion after leaving a current field with an initial velocity u_0 . The family of curves show the effect of varying the initial velocity. For these cases it must be assumed that some aspect of the current or wind force has taken the iceberg from a major current into still water area. Under such conditions the iceberg moves in a spiral pattern and its velocity decays rapidly.

Fig. A-6 shows the iceberg trajectories of small, medium and large icebergs for a similar situation described above and for an initial velocity of 0.25 m/sec in each case.

e) Iceberg Motion in Currents Due to Inertial Oscillations

Fig. A-7 presents the drift of an iceberg with draught less than the depth of the oceanic boundary layer in a rotary current of 12 hrs.

If the iceberg has draught larger than the depth of the oceanic boundary layer, D , the iceberg will be affected by the drag force of the water below the oceanic boundary layer in addition to the rotary current in the boundary layer. If the water under the boundary layer is still, then the size of the loop is greatly reduced as seen in Fig. A-8.



Equations of motion:

$$\frac{dy}{dt} = v' (y_0 - 50) S - r' (y_0 - 50) + \frac{dy}{dt} = v' (y_0 - 50) S + r' (y_0 - 50)$$

$$\text{where } S = \sqrt{(100 - y_0)^2 + (y_0 - 50)^2}$$

FIG. A-1 ANALOG COMPUTER SIMULATION OF ICEBERG MOTION - THE ONE LAYER MODEL

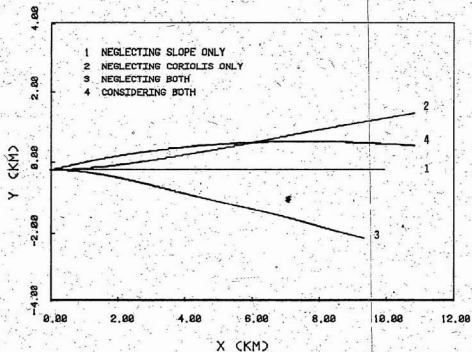


FIG. A-2 EFFECT OF CORIOLIS FORCE AND OCEAN SLOPE ON ICEBERG DRIFT DUE TO GEOSTROPHIC CURRENT OF 0.35 M/S

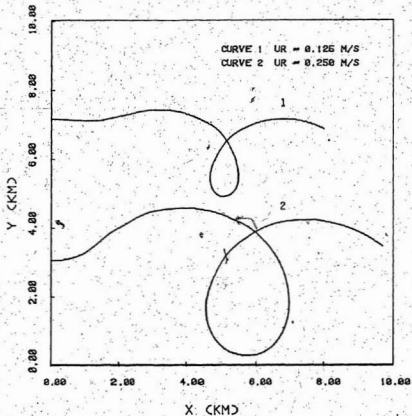


FIG. A-3 ICEBERG DRIFT DUE TO ROTARY CURRENT U_R PLUS A TRANSLATORY COMPONENT OF .085 M/S. PERIOD OF ROTARY CURRENT = 12. HRS.

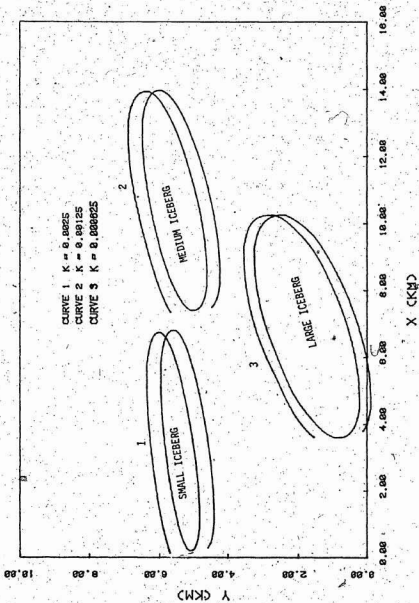


FIG. A-4 ICEBERG DRIFT FOR DIFFERENT VALUES OF K IN A HORIZONTAL CURRENT $U_C = U_0 \sin \text{CMT}$.

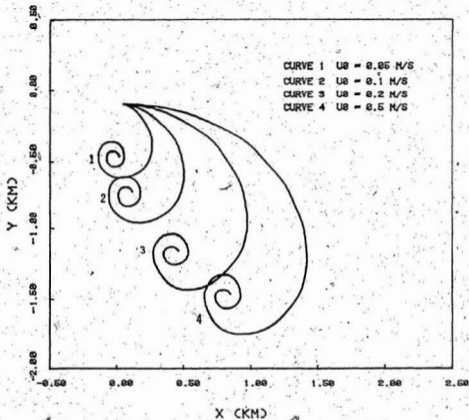


FIG. A-5 ICEBERG DRIFT UNDER CORIOLIS FORCE ONLY
 FOR DIFFERENT INITIAL VELOCITY U_0

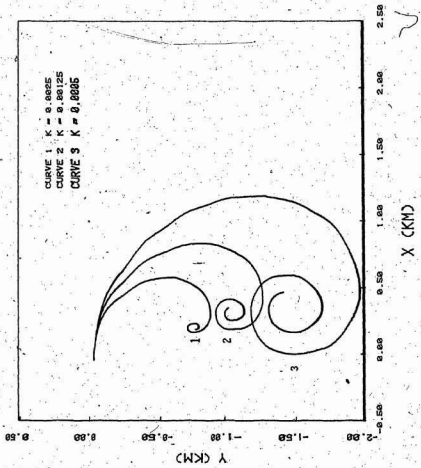


FIG. A-6 EFFECT OF K ON ICEBERG DRIFT UNDER CORIOLIS FORCE ONLY - INITIAL VELOCITY = 0.25 M/S

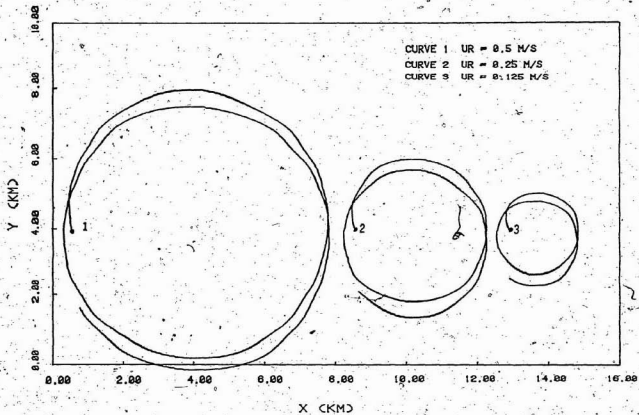


FIG. A-7 ICEBERG-DRIFT DUE TO INERTIAL CURRENT
 CURRENT PERIOD = 12. HRS

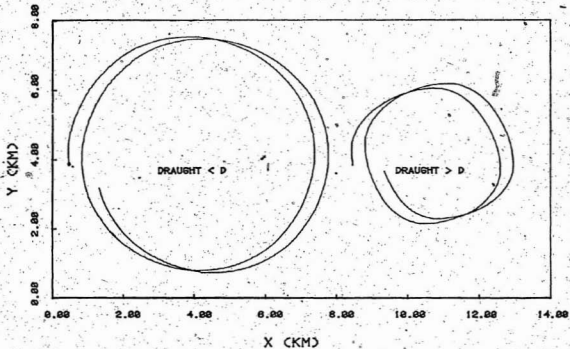


FIG. A-8 ICEBERG DRIFT DUE TO ROTARY CURRENT FOR TWO ICEBERGS WITH DRAUGHT LESS AND GREATER THAN THE DEPTH OF FRICTION LAYER D , $U_R = 0.5$ M/S

APPENDIX B

EFFECT OF ATMOSPHERIC PRESSURE SYSTEM ON OCEAN CURRENTS INDUCED BY CHANGES IN SEA LEVEL

B.1 The Equation of Motion

The continuity equation for a body of water of constant depth h , with surface profile η (+ve downwards; Neumann and Pierson, 1966) is:

$$\frac{\partial u}{\partial x} + \frac{\partial v}{\partial y} = \frac{1}{(h-\eta)} \frac{\partial \eta}{\partial t} \quad (\text{B-1})$$

where:

u is the current velocity in x direction

v is the current velocity in y direction

The factor $(h-\eta)$ can be replaced by h since, usually, $\eta \ll h$, the Eqn.

B.1 can be written in the form:

$$\frac{\partial u}{\partial x} + \frac{\partial v}{\partial y} = \frac{1}{h} \frac{\partial \eta}{\partial t} \quad (\text{B.2})$$

For irrotational flow,

$$u = \frac{\partial \phi}{\partial x} \quad \text{and} \quad v = \frac{\partial \phi}{\partial y} \quad (\text{B.3})$$

where ϕ is the velocity potential.

Substituting from Eqn. B.3 into Eqn. B.2, we get:

$$\frac{\partial^2 \phi}{\partial x^2} + \frac{\partial^2 \phi}{\partial y^2} = \frac{1}{h} \frac{\partial \eta}{\partial t} \quad (\text{B.4})$$

or

$$\nabla^2 \phi = \frac{1}{h} \frac{\partial \eta}{\partial t} \quad (\text{B.5})$$

The boundary conditions of this problem may be prescribed by specifying the values of velocity potential, ϕ , and/or water velocities, u and v ($\frac{\partial \phi}{\partial x}$ and $\frac{\partial \phi}{\partial y}$), at the boundaries.

The finite element technique is used to solve the differential Eqn.

B.5.

B.2 Pressure Distribution

The moving low pressure system is approximated by a function similar to that of two dimensional normal (Gaussian) distribution defined by:

$$\eta(x, y, t) = P_0 e^{-\frac{1}{2}(x - C_x t)^2 / \sigma_x^2} e^{-\frac{1}{2}(y - C_y t)^2 / \sigma_y^2} \quad (\text{B.6})$$

where

η is ocean surface elevation (cm).

P_0 is the peak pressure (mbar).

σ_x and σ_y denote the extent of the pressure system in the x and y directions.

C_x and C_y are the components of the travelling speed of the system.

t is the time.

B.3 Practical Applications

a) Shallow Water

To study the effect of actual low pressure systems on ocean currents, the actual characteristics of the low pressure system that caused the storm over the North Atlantic in the period of August 21-22, 1972 have been used. That low pressure difference of 36 millibar which corresponds to a maximum rise of ocean surface of 36 cm. We assume the

atmospheric pressure distribution to be expressed by expression B.6 which gives reasonably similar pressure distribution to a low pressure system travelling at a fixed velocity.

The F.E. mesh of the 1600 x 1600 km area is presented in Fig. B-1. The centre of the pressure system was assumed to move along x-axis of the model, and the y-axis represents the Labrador Coast. The analysis starts from the moment the (edge of the) pressure system starts to enter the studied area. Since the effect of the pressure system is linear with respect to η/h values (Eqns. B.2 and B.6) it is decided to assume a water depth of 10m ($\eta/h = 0.036$). For other values of η/h , the results can be interpolated.

The results presented in Figs. B-2, B-3 and B-4 indicate that the maximum water velocity occurs under the centre of the pressure system (at the point of maximum surface elevation). Generally speaking, the water particles situated on x-axis moves in a direction parallel to the locus of the pressure centre. The water velocity at the centre depicts the back and forth movement of the waters.

b) Actual Case

The next step is to study the area of the ocean near Saglik, considering the actual profile of the ocean bed and an approximated pressure system (such as given by B.6). The minimum dimension of the F.E. model is taken to be about 1600 km as shown in Fig. B-5 between the Labrador Coast and Greenland. The F.E. discretization, the same as in Fig. B-1, and water depth profile is presented in Fig. B-6. Appropriate boundary conditions are used to simulate the shore at Labrador and Greenland (i.e. zero normal velocity to the shore line) and the open sea in the other two

sides of the F.E. model.

The results presented in Figs. B-7 and B-8 indicate that the effect of the low pressure system on water velocities is negligible due to the large water depth with respect to the peak pressure head. Also it is to be noted that the effect vanishes as the pressure system moves into areas with large water depths.

B.4 Discussion and Conclusion

When a low pressure system passes over an ocean, it raises the ocean surface and causes currents similar in nature to tidal currents. The current velocity is a function of size, traveling speed and the peak value of pressure system. It has been found that the effect of a low pressure system is significant in shallow water (e.g., for water depths less than 20m). Since ocean depth is about 100m in the area near Saglek, it has been found that the changes in current velocities due to the low pressure system is negligible.

The conclusion of this study is that the observed changes in iceberg paths during the storm were not necessarily due to the rise in ocean surface which was caused by the traveling low pressure system.

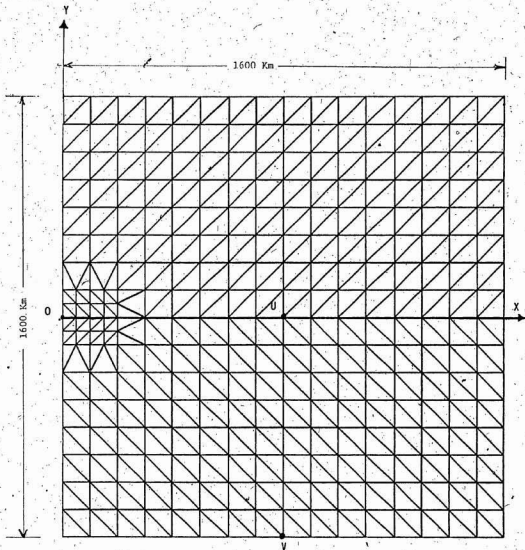


FIG. B-1 FINITE ELEMENT MODEL FOR THE AREA BETWEEN THE LABRADOR COAST AND GREENLAND

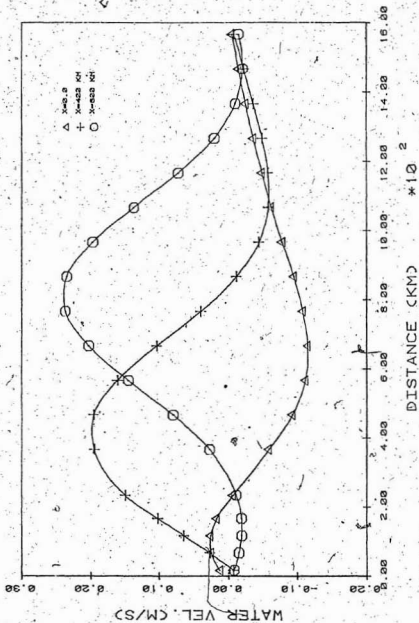


FIG. B-2 DISTRIBUTION OF WATER VEL. ALONG LINE 0-X FOR DIFFERENT POSITIONS OF PRESSURE CENTRE

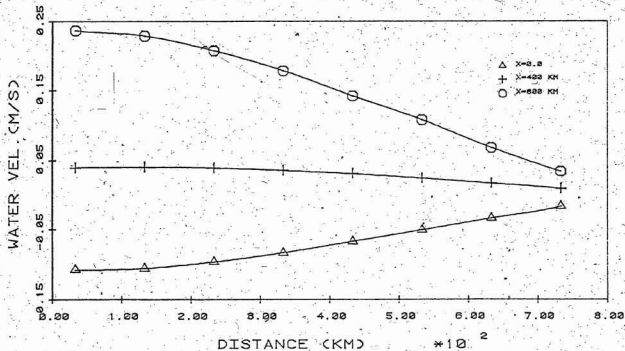


FIG. B-3 DISTRIBUTION OF WATER VEL. AT LINE U-V FOR DIFFERENT POSITIONS OF PRESSURE CENTRE

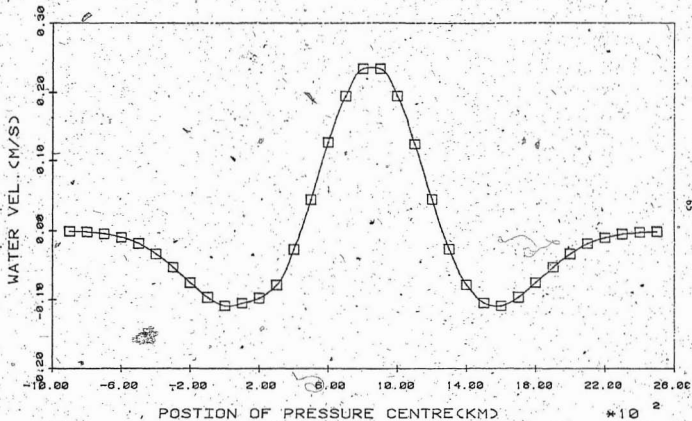


FIG. 8-4 WATER VEL: AT THE CENTRE OF THE AREA VS. POSITION OF PRESSURE CENTRE

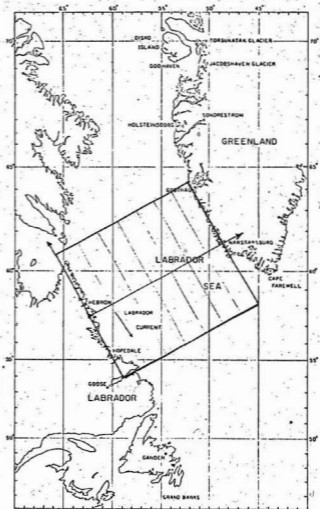


FIG. B-5 LOCATION OF THE STUDY AREA.

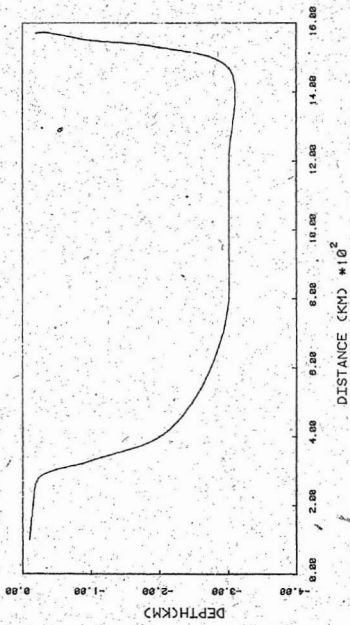


FIG. B-5 DEPTH PROFILE FOR THE STUDIED AREA BETWEEN GREENLAND AND LABRADOR-COAST

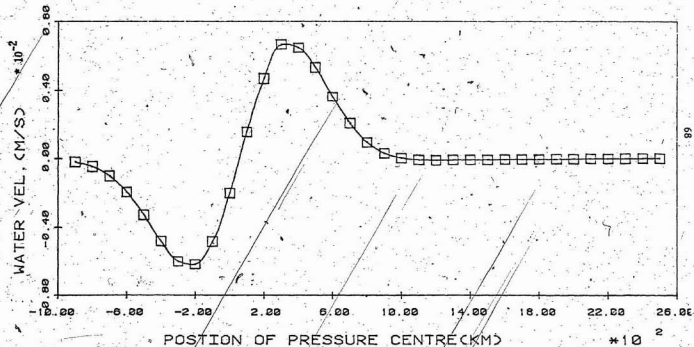


FIG. B-7 WATER VEL. AT OCEAN CURRENT AREA NEAR SAGLEK VS. POSITION OF PRESSURE CENTRE

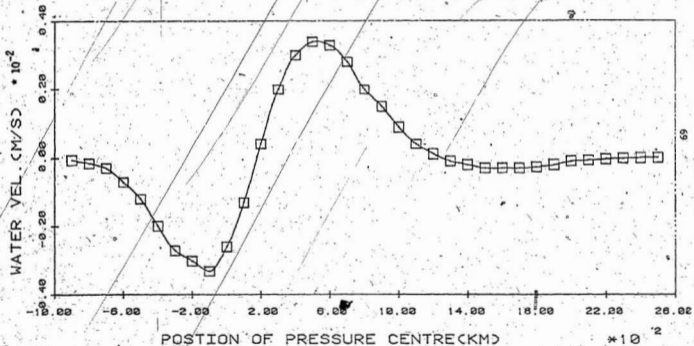


FIG. 8-8 WATER VEL. AT THE MIDDLE OF THE OCEAN
VS. POSITION OF PRESSURE CENTRE

REFERENCES

1. Allen, J.H., (1972), "Iceberg Study, Saglek, Labrador" including "Cruise Report C.S.S. Dawson, August 7 to August 26, 1972", Faculty of Engineering Report, Memorial University of Newfoundland.
2. Banke, E.G. and Smith, S.D. (1974), "Measurement of Towing Drag on Small Icebergs", IEEE International Conference on Engineering in the Ocean Environment, Halifax, Nova Scotia, August 21-23.
3. Bayly, I.M. (1971), "Contribution on the Inclusion of Certain Terms in the Equations Used in the Simulation for the Prediction of Ice Movement by Dr. O. Cochkanoff et al", Canadian Seminar on Icebergs, Halifax.
4. Bruneau, A.A. and Dempster, R.T. (1971), "Iceberg Dynamics", Report submitted to East Coast Petroleum Offshore Association.
5. Cheema, P.S. and Ahuja, H.N. (1978), "Drift of Iceberg in the Grand Banks", Ocean Engineering, Vol. 15.
6. Chirivella, J. and Miller, C (1978), "Hydrodynamics of Icebergs in Transit", Proc. First Int. Conf. on Iceberg Utilization, Ames, Iowa, U.S.A..
7. Cochkanoff, O.; Graham, J.J. and Warner, J.L. (1971), "Simulation Techniques in the Prediction of Iceberg Motion", Proc. Canadian Seminar on Icebergs, Halifax.
8. Dempster, R.T. (1979), "Characteristics of Iceberg Mechanics", IUTAM Symposium on Physics and Mechanics of Ice, Copenhagen, Aug. 6-10.
9. Dempster, R.T. (1974), "The Measurement and Modeling of Iceberg Drift", Proc. IEEE Conf. Ocean 1974, Halifax.
10. Dempster, R.T. and Bruneau, A.A. (1973), "Dangers Presented by Iceberg and Protection Against Them", Arctic Oil and Gas Conference, Le Havre, France, May 2-5.
11. Ertle, R. (1974), "Statistical Analysis of Observed Iceberg Drift", The Fifty-Third Annual Meeting of American Geophysical Union, Washington, D.C..
12. Hamilton, W.S. and Lindell, J.E. (1971), "Fluid Force Analysis and Accelerating Sphere Tests", ASCE, J. Hydraulics Division, June.
13. Hausner, A. (1971), "Analog and Analog/Hybrid Computer Programming", Prentice-Hall, Inc., Englewood Cliffs, N.J..
14. Hoerner, S.F. (1965), "Fluid-Dynamic Drag", Midland Park, New Jersey.
15. Holden, B.J. (1974), "Some Observations on the Labrador Current at

Saglek, Labrador", M. Eng. Project, Faculty of Engineering, Memorial University of Newfoundland.

16. International Ice Patrol (1960), "Wind Effect on Icebergs", Report of the United States Coast Guard.
17. Jenness, R.R. (1965), "Analog Computation and Simulation: Laboratory Approach", Allyn and Bacon, Inc., Boston.
18. Kollymeyer, R.C. (1969); O'Hagan, R.N. and Morse, R.M. (1969), U.S. Coast Guard Rep. No. 10.
19. Lamb, Sir Horace (1879) "Hydrodynamics", Dover Publications, New York, 6th edition, 1932, First published 1879.
20. Mountain, D. (1979), "On Predicting Iceberg Drift", The Iceberg Dynamic Symposium, St. John's, Newfoundland, June 4-5.
21. Murray, J.E. (1969), "The Drift, Deterioration and Distribution of Icebergs in the North Atlantic Ocean", Ice Seminar, Canadian Institute of Mining and Metallurgy.
22. Napoleoni, J.G.P. (1979), "The Dynamics of Iceberg Drift", M.Sc. Thesis, Dept. of Geophysics and Astronomy, Univ. of British Columbia, August.
23. Neumann, G (1968), "Ocean Currents", Elsevier Publishing Company.
24. Neumann and Pierson, W.J. (1966), "Principles of Physical Oceanography", Prentice-Hall.
25. Post, L.A. (1956), "The Role of Gulf Stream in the Prediction of Iceberg Distribution in the North Atlantic", Tellus, Vol. 8.
26. Rekoff, H.G. (1967), "Analog Computer Programming", Charles E. Merrill Books, Inc., Columbus, Ohio.
27. Riggs, N.; Babu, T.; Sullivan, M. and Russell, W.E. (1979), "Analysis of Iceberg Drift Patterns in Lancaster Sound", The Iceberg Dynamics Symposium, St. John's, Newfoundland, June 4-5.
28. Robe, R.Q.; Maier, D.C. and Russell, W.E. (1979), "Long-Term Drift of Icebergs in Baffin Bay and the Labrador Sea", The Iceberg Dynamics Symposium, St. John's, Newfoundland, June 4-5.
29. Russell, W.E.; Riggs, N.P. and Robe, R.Q. (1977), "Local Iceberg Motion - A Comparison of Field and Model Studies", POAC 77, Memorial University of Newfoundland.
30. Russell, W.E. (1973), "Current Studies in the Labrador Current With Respect to the Motion of Icebergs", M. Eng. Thesis, Faculty of Engineering and Applied Science, Memorial University of Newfoundland.

31. Schell, I. (1962), "On the Iceberg Severity of Newfoundland and Its Prediction", Journal of Glaciology, Vol. 4.
32. Smith, E.H. (1931), "The Marion Expedition to Davis Strait and Baffin Bay", Bulletin No. 19, U.S. Treasure Dept., Coast Guard, U.S. Printing Office, Washington.
33. Sodhi, D.S. and Dempster, R.T. (1975), "Motion of Icebergs due to Changes in Water Currents", IEEE Ocean 75.
34. Soulis, E.D. (1976), "Modelling of Iceberg Drift Using Wind and Current Measurements at a Fixed Station", M. Eng. Thesis, Faculty of Engineering and Applied Science, Memorial University of Newfoundland.
35. Weeks, W.F. and Campbell, W.J. (1973), "Towed Icebergs-Plausible or Pipe-dream?", J. Marine Technology Society, Vol. 7, No. 4, August.
36. Zulauf, E.C. and Burnett, J.R. (1966), "Introductory Analog Computation With Graphic Solutions", McGraw Hill Book Company, New York.

